MOLECULAR MECHANISM OF AVEN IN TAXANE INDUCED APOPTOSIS IN ER± BREAST CANCER CELL LINES; MCF-7 AND MDA-MB-231 CELLS

by
AYŞEGÜL VERİM

Submitted to the Graduate School of Engineering and Natural Sciences
in partial fulfilment of
the requirements for the degree of
Master of Science

Sabancı University
June 2006

MOLECULAR MECHANISM OF AVEN IN TAXANE INDUCED APOPTOSIS IN ER± BREAST CANCER CELL LINES; MCF-7 AND MDA-MB-231 CELLS

APPROVED BY:

Prof. Hüveyda Başağa (Thesis Advisor).....

Prof. Zehra Sayers.....

Assoc. Prof. Canan Atılgan.....

Assoc. Prof. Uğur Sezerman.....

Assoc. Prof. Batu Erman .....

Date of Approval: 26.06.2006

ii

MOLECULAR MECHANISM OF AVEN IN TAXANE INDUCED APOPTOSIS IN ER± BREAST CANCER CELL LINES; MCF-7 AND MDA-MB-231 CELLS

Ayşegül VERİM

Biological Sciences and Bioengineering, Master Thesis, 2006

Thesis Supervisor: Prof. Hüveyda Başağa

Key Words: Apoptosis, Taxol, Docetaxel, Aven

ABSTRACT

In this study, the molecular mechanism of Aven in taxane induced apoptosis were studied in ER(+) MCF-7 and ER(-) MDA-MB-231 cell lines. Taxanes, paclitaxel and docetaxel, are cytotoxic agents which act by promoting deformation of stable microtubules, inhibiting the normal dynamic reorganization of microtubule networks required for mitosis.

First the dose kinetics of apoptotic response towards the above mentioned drugs with these two cell lines were established. Cytotoxicity was determined with MTT assay after cells were treated with the drugs for 24 hours. 50nM Paclitaxel treatment for 24h inhibited growth of MCF-7 by 58 percent and MDA-MB-231 by 44 percent.Whereas 50nM Docetaxel caused growth inhibition by 55 percent and 70 percent for 24h in MCF-7 and MDA-MB-231 cell lines respectively. Then Aven protein levels in response to these drugs were studied by western blot analysis. The western blot results showed that Aven protein levels were not changing in response to taxanes in these cell lines. After that the effect of the drugs on protein-protein interaction was investigated with CoIP experiments. Endogeneous Bcl-xL protein was immunoprecipitated with specific Bcl-xL antibody and then immunoblotting was done with anti-Aven antibody. The interaction of Aven with Bcl-xL was not abolished with taxane treatment. The phosphorylation of Bcl-xL with taxane treatment was also shown by western blot analysis. The overexpression of Aven by transfection of both cell lines with pSG-HA-Aven plasmid was performed and then Aven overexpression was checked by western blot analysis. As a control, immunoprecipitation of total protein extract with anti-HA antibody was made. But results showed non-specific binding of endogeneous Aven to HA antibody. As a second strategy, gene silencing was used. Aven expression was downregulated by Hs_Aven_3_HP siRNA in both cell lines. The gene silencing was checked on both RNA and protein level. The mRNA level of Aven was determined first with one step RT PCR and then with quantitative real time RT PCR. The downregulation of Aven was 2.3 fold in MCF-7 cells and 1.7 fold MDA-MB-231 cells. After that, taxane induced apoptotic cell death was investigated by M30 Apoptosense ELISA Kit. The overexpression study showed that taxane induced apoptosis in MCF-7 cells increased by 2 fold. Whereas downregulation of Aven protects MCF-7 cells from apoptosis induced by taxanes. For cisplatin, Aven overexpression resulted in less apoptotic cell death in MCF-7 cells. In MDA-MB-231 cells, overexpression of Aven sensitizes cells for apoptotic cell death.When Aven was downregulated, drugs induced less apoptotic cell death.

ÖSTROJEN RESEPTÖR NEGATİF MCF-7 İLE ÖSTROJEN RESEPTÖR POZİTİF MDA-MB-231 HÜCRELERİNDE TAXANE TARAFINDAN İNDÜKLENEN APOPTOTİK SİNYAL İLETİ YOLAKLARINA AVEN PROTEİNİN ETKİSİ

Ayşegül VERİM

Biyoloji Bilimleri ve Biyomühendislik, Yükseklisans Tezi, 2006

Tez Danışmanı: Prof. Dr. Hüveyda Başağa

Anahtar Kelimeler:Apoptozis, Taxol, Docetaxel, Aven

ÖZET

Bu çalışmada, MCF-7 ile MDA-MB-231 hücrelerinde taxane tarafından indüklenen apoptotik sinyal ileti yolaklarına Aven proteinin etkisi çalışılmıştır.Taxane grubu ilaçlar, hücre icin toksiktirler ve etkilerini mikrotübüller üzerinde göstererek, mitoz için gerekli olan mikrotübül ağının deformasyonuna neden olurlar.

İlk olarak, hücrelere 24 saat ilaç verilerek, sitotoksik etki MTT ile ölçülmüştür. MCF-7 hücrelerine 50 nM paclitaxel verildiğinde hücre çoğalması yüzde 58'e düşerken, MDA-MB-231 hücrelerinde bu düşüş yüzde 44 olmaktadır. Aynı şekilde 50 nM docetaxel verildiğinde hücre çoğalması MCF-7 lerde yüzde 55'e, MDA-MB-231 de ise yüzde 70'e düşmektedir. Optimum ilaç dozunun belirlenmesinden sonra, ilaç verildiğinde Aven proteinin değerindeki değişim immünoblotlama yöntemiyle çalışılmıştır. Sonuçlara göre ilaçlar Aven proteinin seviyesinde bir değişime yol açmamaktadır. Bir sonraki aşamada, taxane grubu ilaçların protein-protein ilişkilerinde herhangi bir değişime neden olup olmadığı ikili immünoçökeltme ile araştırılmıştır. Endojen Bcl-xL proteini immunoçökeltme yöntemiyle çökertilmiş, sonra da Aven antikoru ile immunoblotlanmıştır. İlaçların Aven ile Bcl-xL proteinleri arasındaki interaksiyonu bozmadığı görülmüştür. Bu çalışmada Bcl-xL proteinin fosforile olduğu immunoblotlama yöntemiyle gösterilmiştir. Hücreler pSG-HA-Aven plasmidi ile transfekte edilerek Aven proteinin hücre içersinde daha fazla üretilmesi sağlanmış ve bunu göstermek için immunoblotlama yöntemi kullanılmıştır. Kontrol amaçlı olarak, toplam protein ekstrasından HA antibodisi le immunoçökeltme yapılmıştır. Sonuçlara göre HA antikoru endojen Aven proteinini de getirmektedir. İkinci bir yöntem olaraksa, gen susturma yöntemi kullanılmıştır. Her iki hücrede de Aven seviyesi Hs_Aven_3_HP siRNA ile azaltılmıştır. Genin susturulması hem RNA hem de protein seviyesinde gösterilmiştir. Bir basamaklı ters transkriptaz polimeraz zincir reaksiyonu ve gerçek zamanlı ters transkriptaz polimeraz zincir reaksiyonu kullanılarak mRNA seviyesi kontrol edilmiştir. MCF-7 hücrelerinde Aven seviyesinde 2.3 katlik bir azalma olurken, MDA-MB-231 hücrelerinde bu azalış 1.7 kat olmaktadır.Daha sonra hücrelerdeki apoptoz M30 Apoptoza duyarlı ELISA kitiyle ölçülmüştür. Endojen Aven seviyesindeki artma ile taxane grubu ilaçlar MCF-7 hücrelerini 2 kat daha fazla apoptoza sokmuştur. Öte yandan endojen Aven seviyesindeki azalma, bu hücre tipinde apoptozda azalmaya neden olmuştur. MCF-7 hücrelerine cisplatin verildiğinde, Aven seviyesindeki artmanın daha az apoptoza yol açtığı görülmüştür. MDA-MB-231 hücrelerinde ise Aven seviyesindeki artma taxane grubu ilaçlara karşı hücreleri hassas hale getirmiştir. Hücre içi Aven seviyesi düşürüldüğünde ise, apoptoza gidiş azalmıştır.

To my father, mother and sister...

ACKNOWLEDGEMENTS

This thesis would not have come true without the support of these people. Therefore, I denominate this thesis as ours.

With a deep sense of gratitude, I want to express my sincere appreciation to my advisor, Prof. Hüveyda Başağa for her immense guidance and insight throughout the research. I would like to thank my advisor for her patience, encouragement and enthusiasm and for always being there to encourage me after unsuccessfull experiments.

I am also thankful to Prof. Zehra Sayers, Assoc. Prof. Canan Baysal, Assoc. Prof. Uğur Sezerman and Assoc. Prof. Batu Erman for serving on my committee, spending time in proofreading and constructive comments. I would also like to thank other faculty members, Prof. İsmail Çakmak, Prof. Selim Çetiner, and Assoc. Prof Hikmet Budak for creating such a professional research environment during my education at Sabanci University.

I would like to express my special thanks to Dr. Özgür Kütük, who contributed a lot for this project. He has always been a good friend and helpful researcher who never hesitate to share his knowledge with the ones in need.

I want to express my heartfelt gratefulness to my friends; Elif Damla Arısan in the first place, Dilek Telci, Filiz Dede, Filiz Çollak, Burcu Köktürk, Tuğsan Tezil, Gürkan Yardımcı, Alper Küçükural, Mehmet Alper Arslan, Burcu Kaplan and Özge Cebeci. I would like to thank all my friends in Biological Sciences programs who made my stay at the university a memorable experience. Finally, I would like to express my greatest gratitude to people who gave me the greatest encouragement and motivation to carry out my research work; my father, my mother and my one and only sister. It is a pleasure for me to dedicate this thesis to them.

TABLE OF CONTENTS

LIST OF FIGURES

LIST OF TABLES

LIST OF ABBREVIATIONS

ADP:	Adenosine diphosphate
AIF:	Apoptosis inducing factor
AML:	Acute myeloblastic leukemia
ALL:	Acute lymphoblastic leukemia
Apaf-1:	Apoptosis protease-activating factor-1
ATP:	Adenosine triphosphate
BH1-4:	Bcl-2 homolgy domains
BHK:	Baby hamster kidney
BIR:	Baculovirus IAP repeat
CAD:	Caspase-activated Dnase
Caspase:	Cysteinly aspartate-specific protease
CARD:	Caspase Recruitment Domain
CHO:	Chinese Hamster ovary
c-FLIP:	FLICE-inhibitory protein
CIAP:	Cellular inhibitors of apoptosis
DD:	Death Domain
DED:	Death effector domain
DIABLO:	Direct Inhibitor of apoptosis binding protein with low IP
DISC:	Death-inducing signaling complex
DR:	Death Receptor
ER:	Endoplasmic reticulum
FADD:	Fas-associated death domain
FBS:	Foetal Bovine Serum
HER2:	human epidermal growth factor receptor 2
HtrA2:	High-temperature-requirement protein
IAP:	Inhibitor of apoptosis protein
IL-3:	Interleukin 3

JNK:	c-Jun N-terminal Kinase
MAPK:	Mitogen-activated protein kinase
MBC:	Metastatic breast cancer
MEFs:	Mouse Embryonic Fibroblasts
MTPs:	Mitochondrion permeability transition pores
N-terminus:	Amino terminus
Puma:	p53-up-regulated modulator of apoptosis
SMAC:	Second mitochondria-derived activator of caspases
TNF:	Tumor necrosis factor
TNFR:	Tumor necrosis factor receptor
TRAIL:	TNF-related apoptosis-inducing ligand
TRADD:	Tumor necrosis factor receptor-associated death domain

1 INTRODUCTION

Breast cancer is the most common female cancer, affecting nearly 10% of women at some time during their expected life. Epidemiological studies show that the risk of developing breast cancer increases with age, although younger women tend to present with more aggressive disease. Advanced or metastatic breast cancer (MBC) is currently the second leading cause of death in women after lung cancer and it has been estimated that over 400,000 women worldwide die from the disease each year. MBC is an incurable disease and treatment remains essentially palliative. Although the ultimate goal is to redefine breast cancer as a curable or chronic condition, current therapy can only delay disease progression and improve quality of life. Clinical decisions regarding management of MBC are based on a number of clinicopathological parameters including tumor mass, tumor kinetics, human epidermal growth factor receptor 2 (HER2) status, hormone (estrogen)-receptor status, previous adjuvant therapy, the presence of comorbidities and the time to referral and diagnosis. Chemotherapy with anthracycline- and taxane-based regimens has prayed an important role in increasing life expectancy in women with MBC [1]. Besides the clinical studies for the best therapeutic option, investigation of cellular responses against therapeutic drugs by using human cell lines, gives a huge understanding of how these drugs works and how we can make them more efficient in therapy models.

The taxanes are cytotoxic agents, which have a unique mechanism of action. Thirty years ago, Wani et al., isolated an antitumor agent from the bark of Pacific and needle of European yew trees, Tax*us brevifolia* and *Taxus bacca,* and established its chemical structure—the novel diterpene taxol (Figure 1.1). They act by promoting the formation of stable microtubules inhibiting the normal dynamic reorganisation of microtubule networks required for mitosis and cell proliferation [2]. The two commercially available compounds paclitaxel (Taxol®, Bristol-Meyers-Squibb) and docetaxel (Taxotere®, Aventis) have become recognised as the most active

chemotherapeutic agents in the treatment of advanced breast cancer. They are also used for treatment of multiple types of cancer such as ovarian, lung, head, neck, bladder, and esophagues carcinomas [3].

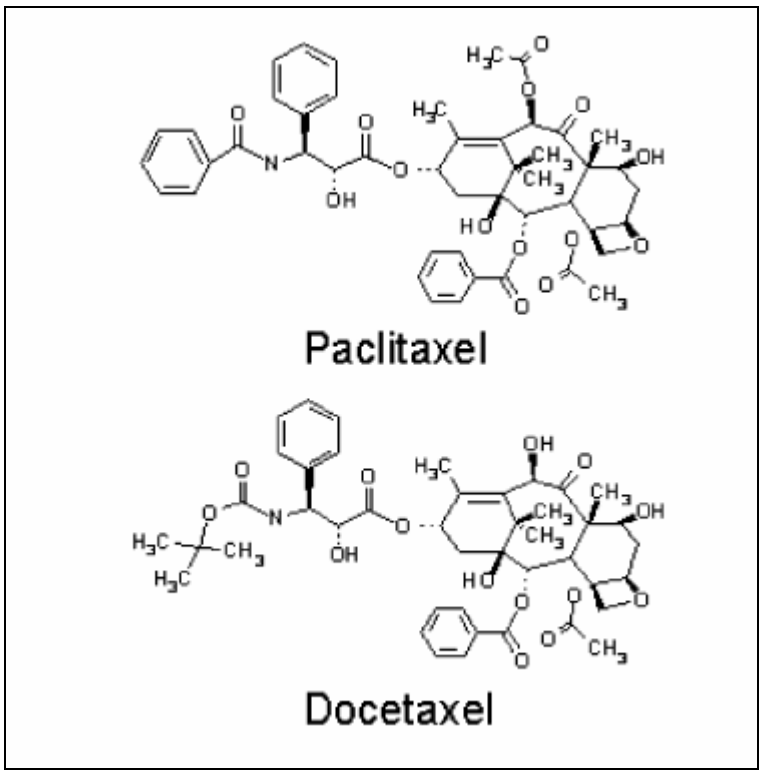

Figure 1. 1 Chemical structures of paclitaxel and docetaxel (modified from [2])

Aberrant mitotic spindle formation caused by taxanes results in cell cycle arrest in G2-M transition between prophase and anaphase of mitosis and leads to cell death at the end [4-7].

Taxanes inhibit the cell proliferation at concentrations lower than those required for microtubule disruption, which infers that there is other action of mechanisms for taxanes. It has been shown that taxanes have numerous biological effects other than microtubule binding, such that phosphorylation of Bcl-2 /Bcl-xl and binding to these anti-apoptotic proteins [8-10], expression of pro-apoptotic genes like Fas/CD95 ligand, activation of transcription factor AP1 [11,12]. There are other apoptosis related proteins such as p53, Bax and caspases, which can be involved in taxane induced apoptotic pathway [13].

Apoptosis is defined by distinct morphological and biochemical changes mediated by a family of cysteinly aspartate-specific proteases (caspases), which are expressed as inactive zymogens and are proteolytically processed to an active state following an apoptotic stimulus. Two separable pathways leading to caspase activation have been characterized [14,15]. The extrinsic pathway is initiated by ligation of transmembrane death receptors (CD95, Tumor necrosis factor(TNF) receptor and TNF-related apoptosis-inducing ligand (TRAIL) receptor to activate membrane-proximal (activator) caspases (caspase-8 and -10), which in turn cleave and activate effector caspases such as caspase-3 and -7. This pathway can be regulated by cellular FLICE-inhibitory protein (cFLIP), which inhibits upstream activator caspases, and inhibitor of apoptosis proteins(IAPs), which affect both activator and effector caspases. The intrinsic pathway requires disruption of the mitochondrial membrane and the release of mitochondrial proteins including Second mitochondria-derived activator of caspases(SMAC) / direct inhibitor of apoptosis-binding protein with low pI (DIABLO) and Omi/HtrA2 (high-temperature-requirement protein), and cytochrome c. Cytochrome c functions with Apoptotic protease activating factor 1 (Apaf 1) to induce activation of caspase-9, thereby initiating the apoptotic caspase cascade, while Smac/DIABLO and HtrA2 bind to and antagonize IAPs [15, 16].

Mitochondrial membrane permeabilization is regulated by the opposing actions of pro- and antiapoptotic Bcl-2 family members. Multidomain proapoptotic Bcl-2 proteins (e.g., Bak and Bax) can be activated directly following interaction with the BH3-only Bcl-2 protein Bid. Alternatively, binding of other BH3-only proteins (e.g., Noxa, p53-up-regulated modulator of apoptosis(PUMA), Bad, and Bim) to antiapoptotic Bcl-2 proteins (e.g., Bcl-2 and Bcl-xL) results in activation of Bax and Bak [17,18]. Whether Bcl-2 proteins control mitochondrial membrane permeability by directly forming pores in the outer membrane, and/or by regulating the opening and closing of the permeability transition pore remains the topic of much debate [19]. The net effect however, is the regulated release of proapoptotic factors from the mitochondria, induction of down-stream caspases, and potential loss of mitochondrial function.

Aven is an anti-apoptotic protein and has been identified by using Bcl-xl mutant 1 (F131V/D133A) as bait in a yeast two hybrid screen of human B-cell cDNA library [20]. This Bcl-xl mutant retains its anti-apoptotic ability but it does not interact with anti-apoptotic proteins such as Bax and Bak. It has been shown that Aven interacts with

Apaf-1 independent of Bcl-xl, transient expression of Aven inhibited proteolytic activation of caspases in cell-free extracts and suppressed apoptosis induced by Apaf-1 and Caspase-9 [20]. It has been also shown that Aven expression together with Bcl-xl stable expression provided enhanced protection of Chinese Hamster ovary (CHO) cells from apoptosis against staurospine exposure, against serum deprivation and against exposure to 4- and 5- day spent medium compare to the parental CHO cells and CHO cells expressing only Bcl-xl alone. Combination of Aven and Bcl-xl has been shown to enhance cell survival [21].

2 BACKGROUND

2.1 APOPTOSIS

2.1.1 Apoptosis Pathways

Apoptosis is of Greek origin, having the meaning ″falling of or dropping off ″ in analogy to leaves falling off trees or petals. Already since the mid-nineteenth century, many observations have indicated that cell death plays a considerable role during physiological processes of multicellular organisms, particularly during embryogenesis and metamorphosis [22, 23]. The term programmed cell death was introduced in 1964, proposing that cell death during development is not of accidental nature but follows a sequence of controlled steps leading to locally and temporally defined self-destruction [24]. Apoptosis is first used by Kerr *et al.* to describe the morphological processes leading to controlled self-distraction [25].

Apoptotic processes are of widespread biological significance, being involved in e.g. development, differentiation, proliferation/homoeostasis, regulation and function of the immune system and in the removal of defect and therefore harmful cells. Thus, dysfunction or dysregulation of the apoptotic program is implicated in a variety of pathological conditions. Defects in apoptosis can result in cancer, autoimmune diseases and spreading of viral infections, while neurodegenerative disorders, AIDS and ischaemic diseases are caused or enhanced by excessive apoptosis [26].

The apoptotic cells have some key features such as blebbing of plasma membrane,

shrinkage of nucleus and cytoplasm, formation of apoptotic bodies containing intact organelles and fragments of nucleus [27]. (Figure 2.1)

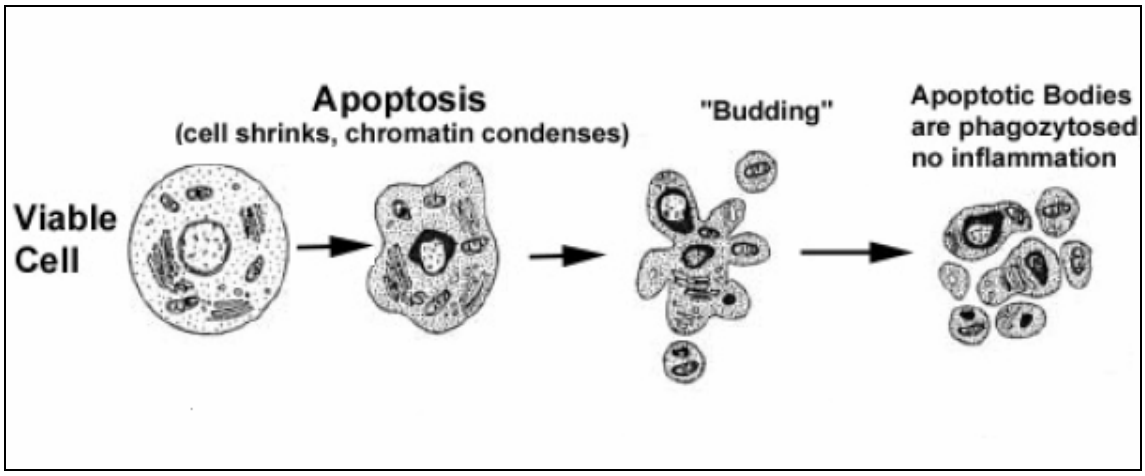

Figure 2. 1 Hallmarks of the apoptotic cell death process. Apoptosis includes cellular shrinking, chromatin condensation and margination at the nuclear periphery with the eventual formation of membrane-bound apoptotic bodies that contain organelles, cytosol and nuclear fragments and are phagocytosed without triggering inflammatory processes. (modified from[29])

Furthermore, with accumulation of reactive oxygen species by mitochondria, the mitochondrial transmembrane potential decreases or acidification of cytoplasm occurs. The change in membrane integrity cause exposure of phosphatidylserine from intracellular space to the extracellular space, which targets apoptotic cells for recognition by the phagocytes and they are degraded by phagocytosis [27]. So they do not cause inflammation. Cells undergo apoptosis upon diverse signals such as withdrawal of growth factors, DNA damage, receptor mediated signals (TNF- or CD95- mediated apoptosis B or T cell receptor- mediated), loss of cellular adhesion, cytotoxic drugs used for cancer therapy.

Main players of apoptotic pathway are first characterized in *Caenorhabditis elegans* [28]. There are four gene products, which are named, as CED-3, CED-4, CED-9 and EGL-1 in *Caenorhabditis elegans*. The death machinery is activated when EGL-1, a proapoptotic BH3-only BCL-2 family homolog, binds CED-9 at the mitochondria and displaces adaptor-protein CED-4 , which then translocates to perinuclear region.

Released CED-4 undergoes oligomerization and it binds to CED-3 leads to formation of a complex defined as an apoptosome in which CED-3 zymogen is activated through close proximity and self-processing [28]. Caspases are evolutionary conserved cysteine proteases, which play an active role in apoptosis. Like other caspases, CED-3 is an inactive zymogen until it undergoes proteolytic activation. This mode of caspase activation is evolutionary conserved. Normally caspases are found in inactive state and they are activated through either death receptor pathway (extrinsic) or through mitochondrial pathway (intrinsic).

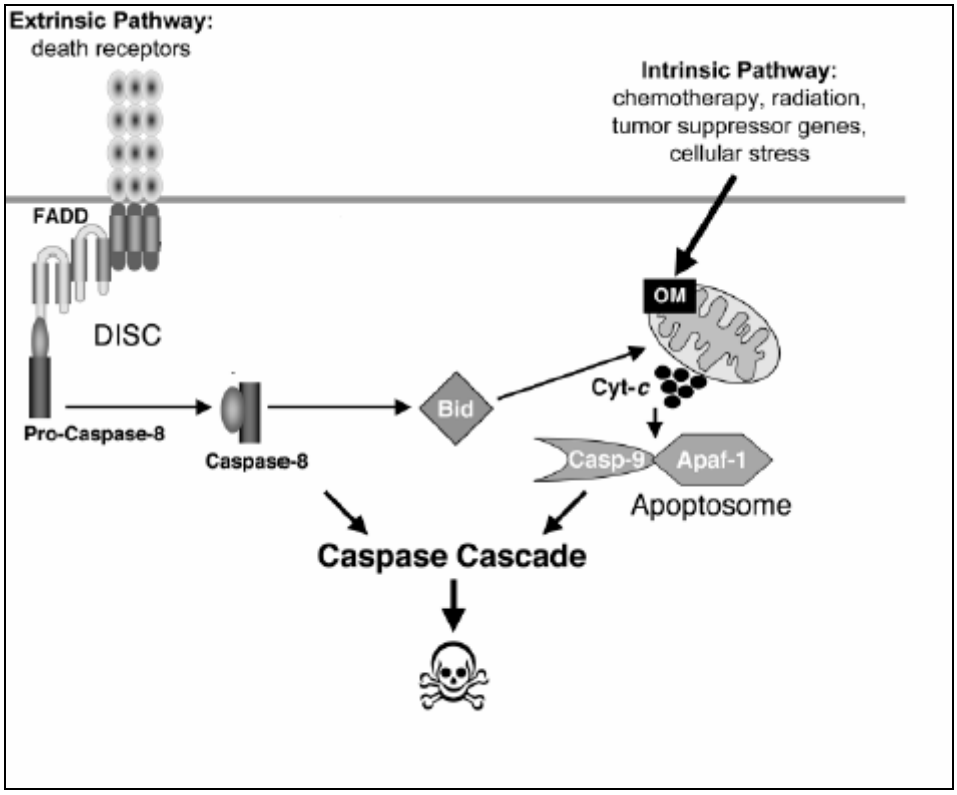

Figure 2. 2 Basic overview of apoptosis pathways (modified from[31])

These two pathways have distinct and overlapping parts and have been identified. They share a couple of adaptor proteins, proteases, protein kinases and protein phosphatases, but how they together regulate survival or death of the cells is not completely known.

In the death receptor pathway that is also called as extrinsic pathway, initiator caspases are activated through adaptor proteins, which are bound to death receptors on the cell surface. The death receptor family members are characterized by the presence of

cysteine-rich repeats in their extracellular domains and protein-protein interaction modules known as the death domain (DD) in their cytoplasmic portions. [30]. Death receptors belong to the tumor necrosis factor receptor (TNFR) gene superfamily, including TNFR-1, Fas/CD95, and the TRAIL receptors DR-4 and DR-5 [32].

Upon binding to their ligands, oligomerization and recruitment of the adaptor proteins occur [30]. For the case of TNF receptor, the adaptor protein is tumor necrosis factor receptor-associated death domain (TRADD) , for Fas receptor it is Fas-associated death domain (FADD). These adaptor proteins recruit procaspases and cause their autoactivation such as procaspase-8 and procaspase-10. Both FADD and TRADD have death effector domain to interact with death effector domains of pro-caspase-8. A massive molecule complex known as the death- inducing signalling complex (DISC) is formed. Within this complex, two linear subunits of pro-caspase-8 compact to each other followed by autoactivation hence caspase-8 formation [33,34,35].

After activation of procaspase-8, the downstream pathway shows a difference in different cell types. In Type-I cells (cells of some lymphoid cell lines), caspase-8 can directly trigger procaspase-3. In Type-II cells (other than Type-I) caspase-8 is mildly activated and cannot activate procaspase-3 [33, 36, 37]. However, it can trigger mitochondrial pathway by truncating Bid (pro-apoptotic member of Bcl-2 family) into its active form tBid. Truncated Bid translocates from cytosol to mitochondria where it oligomerizes with pro-apoptotic Bcl-2 family members Bax and Bak and mediates cytochrome c release [23, 37, 38]. In the cytosol, the released cytochrome c forms a so-called apoptosome complex with the adaptor protein Apaf-1 and pro-caspase-9 in the prescence of dATP. Apoptosome complex is composed of seven Apaf-1 molecules, each bound to one molecule of cytochrome c and a dimer of caspase-9. Within this complex, pro-caspase-9 is activated and triggers the activation of effector caspases, most notably caspase-3, resulting in cleavage of several substrates [37,38].

In the mitochondrial pathway that is also called as intrinsic pathway intracellular death signals cause activation of caspases. This pathway is initiated by receptor-independent apoptotic stimuli such as DNA-damaging agents, kinase inhibitors, hypoxia, growth factor withdrawal, UV and ionizing agents [39-41].

Mitochondria are not only for generation of energy, but also play a role in apoptosis by releasing several pro-apoptotic proteins such as cytochrome c, SMAC/DIABLO and Omi/HtrA2. There are also other proteins which cause caspase-

independent DNA fragmentation and apoptosis-like nuclear morphology such as AIF (apoptosis inducing factor) and endonuclease G, these are also released from mitochondria following apoptosis stimuli [42]. Thus mitochondrial integrity plays an important role since all these apoptotic mediators are kept in mitochondria. The activation of intrinsic pathway and induction of mitochondrial permeabilization are not completely understood, but studies till today provide some hint how apoptotic signals lead to opening of mitochondrion permeability transition pores (MPTPs).

2.1.2 Bcl-2 protein family

2.1.2.1 Multidomain anti-apoptotic Bcl-2 proteins

The Bcl-2 family can be divided into three groups based on their structure and function. Bcl-2, Bcl-xL, Bcl-w, Mcl-1, A1/Bfl-1, Boo/Diva and NR-13 are the multidomain anti-apoptotic ones. They all have four Bcl-2 homology domains (BH1-4), mediating protein-protein interactions, and a hydrophobic C-terminal sequence required for anchoring or insertion in cellular membranes of not only mitochondria but also nucleus and endoplasmic reticulum [43,44]. The α-helices of conserved BH1, BH2 and BH3 domains form a surface exposed hydrophobic groove. This groove constitutes the binding site for BH3 domains of pro-apoptotic proteins. A molecular understanding of this interaction was first revealed by the structure of Bcl-xL bound to a peptide spanning the BH3 domain of Bak, when Bcl-xL complexed with Bak BH3 domain, α-helical BH3 peptide binds in the hydrophobic groove [45].

Not only does the hydrophobic groove bind BH3-only proteins, but it also accommodates the hydrophobic C terminal residues present in multidomain Bcl-2 proteins [46]. Bcl-w and Bcl-xL, which are membrane associated but not predominantly integral membrane proteins in a healthy cell, become more tightly associated with membranes upon interaction with BH3-only proteins [47,48].

Bcl-2 has been shown to act as a regulator for calcium homeostasis or as an antioxidant [49,50]. In addition, Bcl-2 has been shown to prevent the release of the mitochondria activators of the cytosolic caspases as well as the release of cytochrome c. It could also attenuate apoptosis induced by chemotherapy, ionizing radiation and

UV radiation. [40,51,52]. Bcl-2 overexpression protects SW480 cells from TRAIL-induced apoptosis via attenuation of caspase-8 activation and cleavage of Bid and caspase-3 [53]. Whereas Fas-, TNF- and TRAIL- induced apoptosis have been proposed to be insensitive to Bcl-2/Bcl-xL blockage [54,55], therefore the exact mechanism of action of Bcl-2/Bcl-xL in extrinsic pathway remains to be elucidated.

Bcl-2 knockout mice have grey hair, polycystic kidneys and decreased number of lymphocytes [56], Bcl-xL knockout mice die at around day 13 of gestation due to massive neuronal and hematopoetic apoptosis [57]. Post-translational modifications such as phosphorylation and cleavage also play an important role for regulation of Bcl-2 and Bcl-xL activity. PKC phosphorylation of Bcl-2 at Ser-70 has been shown to be required for efficient anti-apoptotic function [58].

In contrast, microtubuli-targeting agents such as paclitaxel induce hyperphosphorylation of Bcl-2 (Ser-70, Ser-87, and Thr-69) and prevent its anti-apoptotic function [59]. Phosphorylation of Bcl-xL at Ser-62 by JNK (c-Jun N-terminal kinase) in response to taxol has been reported to oppose the anti-apoptotic function of Bcl-xL and sensitizes prostate cancer cells to apoptosis [60]. The caspase-dependent N-terminal cleavage of Bcl-2/Bcl-xL and exposure of their BH3 domains converts into pro-apoptotic ones.

2.1.2.2 Multidomain pro-apoptotic members of Bcl-2 proteins

Bax, Bak and Bok/Mtd are the members of the second group. Bax is mainly cytosolic and loosely associated to the outer membrane of mitochondria or ER as a monomer. Upon apoptotic stimuli, Bax undergoes a unique conformational change exposing its C-terminal hydrophobic domain, which is required for mitochondrial anchorage [61]. It forms dimers, oligomers, or higher-order multimers in the mitochondrial membrane [62]. Bak is another member of this family and it is associated to outer mitochondrial membrane and ER. Bak also undergoes conformational change upon apoptotic stimuli such as etoposide and cisplatin [63, 64]. Bak-/- Bax-/- mouse embryonic fibroblasts (MEFs) has been shown to be insensitive to multiple apoptotic stimuli including chemotherapeutics and UV radiation [65]. The requirement of Bak and Bax in the apoptosis has been confirmed by other studies.

Bax-null cells have been shown to be resistant to TRAIL-induced apoptosis [66]. Caspase-8 activation and Bid-cleavage by TRAIL can occur in Bax deficiency, whereas the release of Smac/DIABLO, which causes inhibition of IAP proteins and activation of caspase-3 was abrogated [66]. In a recent study, it has been shown that activation of multiple caspases by DNA damage and ER stress has been directly regulated by Bax and Bak in double knockout MEFs [67].

Bax or Bak activity is also regulated by post-translational modifications such as cleavage. Calpain-mediated conversion of Bax into truncated form (arises from cleavage of N-terminal 33 amino acids, p18 Bax) enhances its pro-apoptotic activity upon stimulation with chemotherapeutics [68]. The truncated Bax behaves lile BH-3 only protein and sensitivity to apoptosis by p18 Bax has been proposed to be related to increased affinity for Bcl-xL. It has been also shown that a cathepsin-like cysteine protease is involved in degradation of p18 Bax and stabilization of p18 Bax by cathepsin inhibitors enhances drug-induced apoptosis [69].

2.1.2.3 BH3-only anti-apoptotic Bcl-2 proteins

Third group is formed by the BH3-only proteins (Bid, Bad, Bim, Hrk, Blk, Bik, Noxa, Puma, BNIP3, Nix and BMF) that only share homology in a stretch of 9–16 amino acids called the BH3 motif mainly act through inhibition of Bcl2/Bcl-xL and activation of Bak and Bax. It has been suggested that BH3-only members function as death sensors, where various death stimuli seem to activate different BH3-only proteins. They coordinate fine-tuning of apoptotic response through their interactions with pro- and anti-apoptotic members, but the definitive mechanism that lie behind remain to be clarified [70]. There are two main ways, which BH3-only proteins function on mitochondria. Some of them (Bid and Bim) function through interacting with pro-apoptotic Bcl-2 proteins such as Bax and Bak and induce their activation/oligomerization. These are called as direct activators and they can be attenuated by Bcl-2 through selective sequestration and functional silencing. Other BH3-only members (Bad) interact with anti-apoptotic Bcl-2 members and prevent them binding and sequestering BH3-only proteins such as Bid and Bim thereby Bax and Bak activation can occur. They are called as sensitizers.

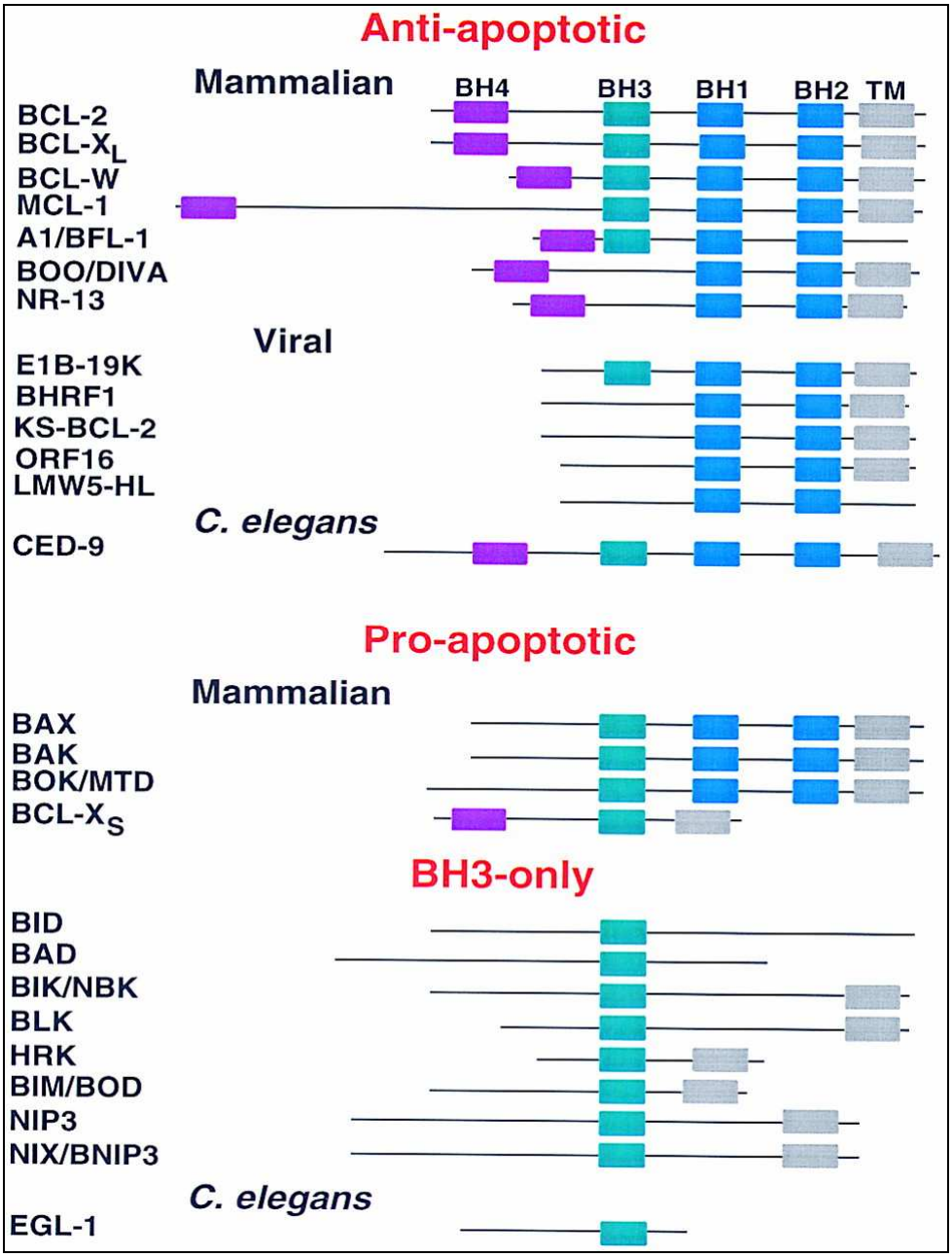

Figure 2. 3 Bcl-2 protein family members.(modified from[81])

BH3-only proteins are regulated by a wide range of mechanisms at the mRNA as well as at the protein level, including post-translational modifications and sequestration in cellular structures.

1) Transcriptional regulation of BH3-only proteins

Puma (p53 up-regulated modulator of apoptosis) and Noxa are transcriptional targets for p53 [71,72]. Upon induction of apoptosis by chemotherapeutics such **5**-fluorouracil (5-FU) PUMA is transcriptionally induced and localized to mitochondria, where it associates with Bcl-2 and Bcl-xL, thereby inducing cytochrome c release as well as caspase-9 and caspase-3 activation [73]. Increased expression of Noxa mRNA and protein in response to x-ray irradiation has been demonstrated in wild-type thymocytes, but not in p53-deficient thymocytes. Noxa translocates to the mitochondria and interacts with Bcl-2 and Bcl-xL, leading to a decrease in mitochondrial membrane potential and cytochrome c release [72].

2) Control by phosphorylation

Selective phosphorylation of proteins at different residues may control different molecular and cellular responses. The proapoptotic function of Bad is regulated by its phosphorylation status. Phosphorylation of Bad at Ser-112, Ser136 and Ser-155 has been described upon stimulation of cells with different growth factors, such as PDGF, NGF, IL-3, IL-2 or IL-4 [74]. The result of these phosphorylation events is the binding of Bad to the cytoplasmic protein 14-3-3, avoiding its interaction with Bcl-2 and Bcl-xL and allowing survival of the cells [74,75].

Recently, two more phosphorylation sites have been identified: ser128 and ser170. The phosphorylation at ser170 blocks the proapoptotic activity of Bad, but does not avoid Bad/Bcl-xL interaction. Interestingly, ser128 is phosphorylated in cerebellar granule neurons upon apoptotic stimuli by cdc2, inhibiting the interaction of Bad with 14-3-3 and promoting the apoptotic activity of Bad [76,77,78]. Bik is phosphorylated at serine 35 and threonine 33 by a kinase related to casein kinase II (CKII). These phosphorylations are required for an efficient Bik-mediated cell death, although they do not affect the interaction between Bik and Bcl-2 [79].

3) Regulation by proteolysis

There are many proteins implicated in apoptosis that are activated or inactivated by proteolysis, including some BH3-only proteins. In healthy cells the protein Bid remains in the cytosol and different apoptotic signals induce its cleavage and translocation of the truncated protein (tBid) to the mitochondria, where it promotes the exit of cytochrome *c*. After the activation of cell-surface death receptors, such as Fas and TNF-a, caspase-8 is activated and cleaves Bid, generating two fragments [80,81]. The carboxyl terminal fragment (tBid) has a newly exposed glycine residue that is myristoylated, and targets tBid to the mitochondria [82].

2.1.3 Caspases

As their name implies they cleave substrates on the carboxyl site of aspartate and bear catalytic cysteine residue in their conserved pentapeptide active-site 'QACXG' (X can be R , Q or D) and their precursors are zymogens known as procaspases [83]. Procaspases posses a large and a small subunit preceeding with an N-terminal prodomain which is required for activation. They have the ability of autoactivating as well as activating other caspases. In order to be activated two cleavages occurs in two aspartic acids, then small and large subunits come together to generate the active site of the enzyme. Active enzyme is composed of two heterodimers hence it is a tetramer containing two active sites [84].

To date fourteen members have been identified in humans and named as Caspase-1, -2, -3, -4, -5, -6, -7, -8, -9, -10, -11, -12, -13 and –14. Caspases can be divided into two groups with respect to their structure. Caspases with long prodomain have structural motifs such as caspase activation and recruitment domain (CARD) or death effector domains (DEDs) which enables them to interact with other proteins. These three domains share a common 3D structure known as death domain fold, composed of six anti-parallel α-helices arranged in a Greek key conformation [85]. Second group of caspases have short prodomains and they are activated with proteolytic cleavege by other caspases. Caspases-1, -2, -4, -5, -8, -9, -10, -11, -12, -13 and -14 belong to former group whereas Caspases -3, -6, -7 and -14 are in the second group. Caspases can also be grouped based on their function as apoptotic or inflammatory.

Caspases -1, -4, -5, and -11 , -12, -13 have been shown to play role during cytokine maturation and inflamation. Other members have apoptotic effects. The apoptotic group can be subdivided into two as initiator caspases (caspases -2, -8, -9, -10, -12) or effector caspases (caspases –3, -6, -7, -14). Initiator caspases are on the upstream of the apoptotic pathway. They activate effector caspases with different mechanisms. They could directly interact and cleave effector caspases or interact indirectly through another messenger mechanism. Upon activation via initiator caspases, effector caspases cleaves many substrates and cause cell death. Since initiator caspases have short prodomain whereas effector caspases bear long prodomain.

The processing and activation of caspases are of major importance for apoptotic signaling. However, a processed caspase is not always catalytically active, as their activity and processing are under the control of IAPs.

2.1.4 Regulation of apoptosis by IAPs

IAPs are a family of antiapoptotic proteins whose prototype originally was described in baculovirus with many homologues found to be conserved across several species. All IAPs contain baculovirus IAP repeat (BIR) domains, 70 amino acid motifs, which are essential for the antiapoptotic properties of IAPs [86], because it is the interaction between the BIR domains and caspases that is believed to confer most of the antiapoptotic activity of IAPs. Indeed, XIAP, c-IAP1 and c-IAP2 are thought to directly inhibit caspases-3, -7, and –9 [87]. In case of XIAP, it is the BIR3 domain that directly binds to the small subunit of caspase-9, whereas it is the BIR2 domain that interacts with the active-site substrate-binding pocket of caspases-3 and –7 [88,89]. In addition to the BIR domains, c-IAP1, c-IAP2, and XIAP contain a highly conserved RING domain at their C-terminal end, which possesses E3 ubiquitin ligase activity. Via this RING domain, IAPs are able to catalyze their own ubiquitination, thereby targeting themselves for degradation by the proteasome [90], but they also might target other proteins such as caspase-3 and –7 for ubiquitination and degradation [91,92]. Cells overexpressing mutant XIAP lacking the RING domain were characterized by resistance in proteosome-mediated degradation and low level of apoptosis as compared with those expressing wild-type XIAP [90].

Direct inhibition of caspase activity by c-IAPs is certainly a very important means

of regulation when considered that signaling cascades mediated by proteolytic enzymes such as caspases is irreversible once activated and therefore must be precisely regulated in order to prevent locally and temporally inappropriate demise of cells.

The mitochondria-localized proteins Smac/DIABLO and HtrA2/Omi antagonize the effect of IAPs. Both these proteins contain an IAP-binding motif and therefore they neutralize anti-apoptotic effect of IAPs [93,94]. Thus within cells a balance between expression of IAPs and Smac/DIABLO and HtrA2/Omi may determine whether a certain apoptotic stimuli will trigger apoptosis.

2.1.5 Aven

Aven is an anti-apoptotic protein and discovered in yeast two hybrid screen by Chau et al, 2000 [20]. Expression of Aven mRNA was detected in a wide variety of adult tissues and cell lines and homologs of Aven were found in mouse, rat, and rabbit EST databases. Indirect immunofluorescence of baby hamster kidney (BHK) cells has revealed a diffuse nuclear staining pattern and a reticular cytoplasmic staining pattern consistent with intracellular membrane localization. Also, cells transiently cotransfected with Aven and Bcl-xL revealed that some, but not all, of the Aven and Bcl-xL colocalized [20]. Aven was found to interact with anti-apoptotic Bcl-2 family members in immunoprecipitation studies, but the protein did not interact with pro-apoptotic Bcl-2 family members or members that had lost their function. It has been shown that, Aven expressed transiently provides protection from apoptosis stimuli such as interleukin-3 (IL-3) withdrawal and γ-irradiation in FL5.12 cells, and in vivo Sindbis virus intracerebral injection in mice [20].

It has been shown that Aven interacts with Apaf-1, a mammalian homolog of CED-4. It interacts independently with both Bcl-xL and Apaf-1 [20]. However, in vitro-translated proteins did not provide detectable interactions between Aven and Apaf-1, which suggests that other cellular factor(s) and/or posttranslational modifications are essential for their interaction. There was also evidence that Aven is involved in inhibiting the activation of the initiator, caspase-9. Aven expressed transiently in 293,

Table 2.1. Bcl-2 family members interacting or not interacting with Aven as determined by Chau et al. (2000).

Bcl-2 family members	Pro- or Anti-apoptotic	Interaction with Aven
Bax	Pro-	No
Bak	Pro-	No
hBcl-2	Anti-	Yes
hBcl-xL	Anti-	Yes
KSBcl-2	Anti-	Yes
Bcl-xL(Δ26-83)	Anti-	Yes
Bcl-xL(ΔN61)	Pro-	No
Bcl-xL mt 1	Anti-	Yes
Bcl-xL mt 7 (V135A/N1361/W137L)	Nonfunctional	No

BHK, and MCF-7 cells blocked cell death mediated by the cotransfection of Apaf-1 and caspase-9. Aven mediated its protective function without inducing or promoting the degradation of either Apaf-1 or caspase-9 [20]. The inhibition of Apaf-1-mediated cell death suggests that Aven interferes with the interaction of procaspase-9 and Apaf-1 or at another step in apoptosome activation cascade. Aven was also shown to impair the autoprocessing of caspase-9 after the addition of cytochrome c and dATP to cell extracts. In addition, Aven inhibited the processing of caspase-3, which suggests that impaired activation of caspase-9 results in the failure of caspase-9 to activate caspase-3 [20].

It has been shown that stable expression of Aven in CHO cells provided limited protection against staurosporine treatment [21]. Aven was also found to provide protection after exposure to serum deprivation and spent medium during the early batch growth phases (4- and 5-day) [21]. However Aven expression was observed to be pro-apoptotic after Sindbis virus infection of CHO cell cultures [21]. When both Bcl-xL and Aven were expressed together , it has been observed to be an enhanced protection relative to CHO bcl-xL, CHO-aven, and the parental CHO cell line under serum deprivation and after exposure to both 4- and 5- day spent medium. Whereas expression of Aven and Bcl-xL has shown to be lowering the viabilities at 2 days post-infection after Sindbis virus infection [21].

Paydas et al. showed that Aven expression is higher in patients with acute myeloblastic leukemia (AML) and acute lymphoblastic leukemia (ALL) compare to the controls (P=0.035). They also showed that Aven was higher in patients with relapse as compared with non-relapse patients ($P = 0.04$) [95].

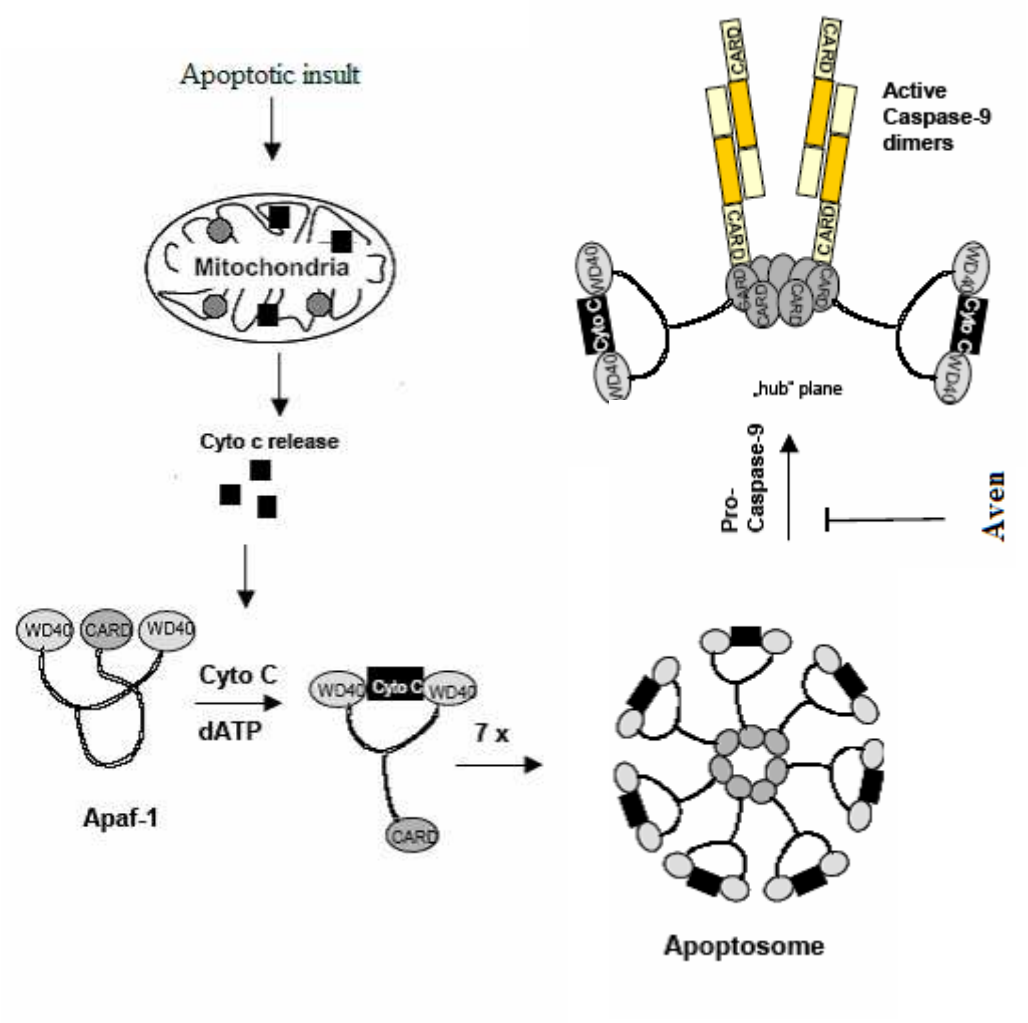

Figure 2. 4 Apoptosome complex formation and possible mechanism of action for Aven. (modified from [29])

2.1.6 Taxanes

2.1.6.1 Apoptotic cell death induction by taxanes

Paclitaxel binds specifically to microtubules, promotes the re-organization of the microtubular network into bundles or asters and stabilizes microtubules against disruption by various agents. Docetaxel produces similar effects, it is more potent on a molar basis in inhibiting microtubulin depolymerisation than paclitaxel [96].

By stabilizing spindle microtubules in the absence of GTP, taxanes block cell cycle progression through the G2-M phase [97, 98]. Moreover, docetaxel inhibits chromosomal segregation and polarization during this mitotic phase [99]. As predicted by their biochemical mechanism of action, these mitotic inhibitors not only affect the undergoing cellular mitosis, but exert cytoskeleton disruption. Thus, immobilization of the spindles inhibits cellular trafficking, which probably restricts DNA repair mechanism, and therefore forcing cells to the commitment of cell death. [3,100].

Apoptosis induced by paclitaxel and docetaxel is a complex process associated with various signal transduction pathways (as illustrated in Fig.2.5). For instance, paclitaxel and docetaxel induced major hyperphosphorylation of Bcl-2 which abolishes its anti-apoptotic function during mitotic arrest. Yet, anti-apoptotic effects of Bcl-2 are important only in apoptosis-prone cells. Nevertheless, taxanes cause either apoptotic or post-mitotic cell death (delayed cell death) depending on the tumor cell type.

Furthermore, mitochondria and other intracellular organelles seem to interact with microtubular compounds and may be transported *via* microtubule-dependent motor proteins [101]. Thus, microtubule-stabilizing agents, which induced microtubule nucleation with random orientations throughout the cytoplasm, could directly perturb mitochondrial network and re-distribution during cell division. One direct consequence of this phenomenon is a dispersed distribution of mitochondria. It appears that mitochondria and their membrane permeability play a crucial role in the apoptotic program initiation after paclitaxel or docetaxel addition. Mitochondria and other organelles appear to be apoptotic death sensors after taxanes exposure by stimulating unique and/or common caspase- and non-caspase-activating complexes. Thus, signal transduction pathway of apoptosis could also vary according to the nature of cancer cell

lines. Furthermore, recent findings agree on that cancer cell lines have more than one way to die after chemotherapeutic treatment. The mechanism underlying apoptosis induction by microtubule-interacting agents differs in some respect from that of other anticancer drugs and could involve pro-apoptotic factors interacting with microtubular proteins, such as Bim. On the other side, Bim activation has been described as a possible candidate in apoptosis induced by ionizing radiation. Taken together, this information suggest that the triggering of distinct cell death (apoptosis or necrosis) pathways might be dependent on both the tumor cell-type and the anti-mitotic agent used . So, understanding of signal transduction pathways and different biological effects may reveal different avenues in cell death induction by docetaxel and paclitaxel that would be useful in anticancer therapies.

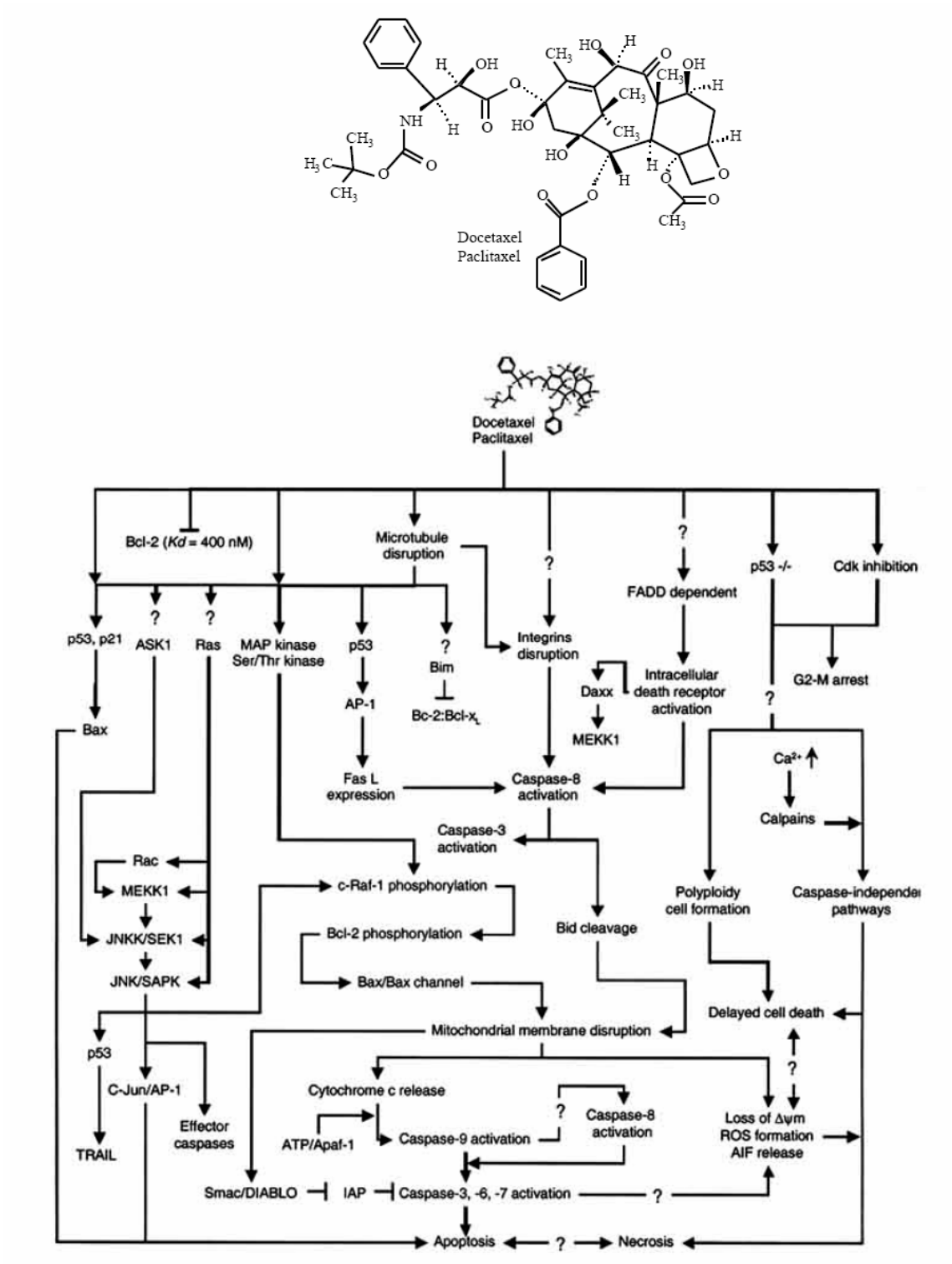

Figure 2. 5 The signal transduction pathway induced by taxanes (modified from [169])

2.1.6.3 Bcl-2 Phosphorylation by Taxanes

The inactivation of Bcl-2 proteins by serine-phosphorylation has been shown to play a pivotal role in taxane-induced apoptosis [8, 102]. Several studies have demonstrated drugs targeting microtubules could induce Bcl-2 phosphorylation, whereas this action is not seen by DNA damaging agents [9]. Human lymphoma, breast cancer and prostate cancer cells exposed to paclitaxel undergo apoptosis [8], in correlation with the appearance of a phosphorylated form of Bcl-2, suggesting that the phosphorylation of this anti-apoptotic protein may inhibit its function. Several kinases have been proposed as Bcl-2 kinases so far. Raf-1 kinase, PKC, PKA, JNK and cdc2 kinase all phosphorylate Bcl-2 protein at different sites and with distinct effects on its kinetics [102]. These kinases might be activated partly by drug stimuli or in a cell cycle-dependent manner [103].

The phosphorylation of Bcl-2 at serine residues has been shown to interfere with the anti-apoptotic function of Bcl-2 by preventing Bcl-2 binding to pro-apoptotic Bax protein [10]. So, antimicrotubule agents are potent inducers of Bcl-2 phosphorylation and inhibitor of the anti-apoptotic function of this protein [8, 104, 105]. Moreover, it has been indicated that docetaxel is a more potent inducer of Bcl-2 phosphorylation than paclitaxel [104].

On an other hand, stabilization of microtubules by taxanes results in inactivation of Bcl-2 member proteins, leading to increase in Bax protein levels and resulting in apoptosis [9, 106]. On induction of apoptosis, Bim pro-apoptotic Bcl-2 family member can translocate from microtubuli to mitochondria, where the latter incorporate into the outer membrane, in association with Bax protein, and may undergo a conformational change [107], which could modified the mitochondrial PTP and initiated the apical caspase-9 activation by cytochrome c release. So, inactivation of Bcl-2 is achieved by taxanes, which act on microtubule assembly and cause its hyperphosphorylation [108] and, simultaneously, favor opening of the mitochondrial permeability transition pore [109], and the triggering of the apoptosome complex activation. Indeed, Bcl-2 may be viewed as a direct molecular target of taxanes.

Lui and Stein have reported that paclitaxel-treated LNCaP cells induced alteration in Bcl-xL and Bak level expression [110]. Whereas, docetaxel does not induce any

change in the levels of Bcl-2, Bak, or c-myc protein expression [104]. It has been also shown that introduction of *bax* gene increased the cytotoxicity of different anticancer agents such as paclitaxel, vincristine and doxorubicin in ovarian SW626 cancer cells [111]. It has been suggested that *bax* gene was transcriptionally activated by the presence of p53 as a downstream target gene in apoptosis.

These findings support that taxanes-induced apoptosis can be regulated by up-regulation of such pro-apoptotic genes and down-regulation of anti-apoptotic genes. The molecular regulation appears more complex in cancer cell lines, because of their different status in apoptotic genes expression. Thus, signal transduction pathways leading to apoptosis by microtubule stabilizing agents is also involved in pro-apoptotic genes activation [112], such as *bax,* and certainly other unidentified genes. It has been reported that all paclitaxel-induced cellular effects were abrogated by the protein synthesis inhibitor, cycloheximide and the RNA synthesis inhibitor, actinomycin D [113], suggesting that pro-apoptotic signal transcription is also an important step of apoptosis induction by taxanes. Nevertheless, the mechanism whereby taxane impair Bcl member protein expression is not well elucidated.

2.1.6.4 Caspase Cascades involved in Taxane induced apoptosis

It has been shown that docetaxel induces concentration dependent apoptotic cell-death. In docetaxel-treated cells both necrotic and apoptotic cell death have been observed. Treatment of L929 cells with caspase-1 inhibitors and caspase-3 inhibitors results in abrogation of docetaxel-induced DNA fragmentation. This shows that both caspase families are involved in docetaxel-induced apoptosis. Moreover, caspases, especially these two subfamilies, act certainly as common mediators of apoptotic and necrotic cell death and play major role in signal transduction pathway initiated by a panel of chemotherapeutic agents [114]. It has recently been identified that mitochondrial membrane permeability is a key to the decision step between apoptosis and necrosis. These two modes of cell death represent different execution sub-routines of the same death program, while necrosis is viewed as the result of an incomplete execution of apoptosis [115]. Caspase inhibition in combination with taxanes did not change cell viability loss. Nevertheless caspase inhibition was shown to prevent caspase-activated DNase (CAD), which once activated lead to internucleosomal DNA

fragmentation. It has been shown that apoptosis inhibition leads to necrotic cell death, suggesting that caspase orients the cell death in DNA damaged cancer cells after genotoxic insults. Caspase inhibitors cannot totally block the release of cytochrome c and the perturbation of mitochondrial membrane potential [116,117]. Membrane potential permeability of mitochondria is not only regulated by caspases, but also by different pro-apoptotic members of Bcl-2 family such as Bax and/or Bid proteins and certainly other unknown actors. Moreover, apoptotic cell death in breast MCF-7 cancer cells, which are deficient in caspase-3, can be induced by taxanes [118]. In this regard, docetaxel can induce apoptosis by various apoptotic signal transduction pathways, which are also caspase-3-independent. Suggesting that other proteases or undiscovered caspases are involved in apoptosis induced by this mitotic poison agent. A recent study has considered that caspase-8-mediated processing of nuclear procaspase-9 requires the participation of caspase-3-like activity in caspase-3-deficient MCF-7 cells [119]. Caspase effector such as caspase-7 could be a second candidate to assume the caspase-3 role in apoptosis. Nevertheless, Kaufmann Scott and colleagues have recently demonstrated that caspase-7 is unable to cleave the caspase-3-dependent proteolytic substrates in MCF-7 deficient caspase-3 cells [120].

Activation of effector pro-caspases, such as pro-caspase-3 and -7 has been shown with paclitaxel, leading to apoptotic hallmarks [121, 122]. However, little is known about initiator caspases, which are involved in taxanes-induced apoptosis. A recent finding has indicated that paclitaxel and other anti-microtubule agents induced apoptosis in the human colon cancer HT29-D4 cell line (which does not express Bcl-2 protein) following mitotic block, Bcl-xL phosphorylation (which may be a substitute for Bcl-2 when the latter is not expressed), loss of mitochondrial transmembrane potential and caspase-8 activation [123]. A recent report showed that TRAIL, Fas-L and anti-DR5 antibody increased apoptosis induced by paclitaxel in human nonsmall-cell lung cancer [124], suggesting that apoptotic death domain receptors may also participate in this active cell death by amplifying classical caspase-dependent apoptotic cascade.

Caspase-8 can act either up-stream or downstream of mitochondria pathway induced apoptosis [125]. After 72 hour paclitaxel-treatment in HT29-D4 cells, mitochondrial membrane potential was reduced for the concentrations which induced

mitotic block and Bcl-xL phosphorylation, concomitantly to caspase-8 activation [123]. In contrast, other studies have described Fas-L up regulation after paclitaxel treatment and partial inhibition of apoptosis by using Fas-L-neutralizing and/or Fas-blocking antibody, suggesting that this mitotic inhibitor induced an autocrine or paracrine type of apoptosis by a Fas-dependent pathway [126, 127]. Such divergent results indicate that Fas ligation involvement in paclitaxel-induced apoptosis is dispensable since it may vary according to the cell type.

Antimitotic agents might activate factors regulating Fas-mediated apoptosis independently of Fas ligation, which results in caspase-8 activation. Indeed, the alteration of mitochondrial membranes permeability leads to apoptotic cell death (and in a certain extent to necrosis) by cytosolic release of pro-apoptotic proteins, such as pro-caspase-2, -3 and -9, AIF and/or cytochrome c that may activate caspase-8 [125, 126]. In paclitaxel-treated U937 cells, occurrence of mitochondrial dysfunction, cytosolic accumulation of cytochrome c, cleavage of pro-caspase-9 and subsequent cleavage of pro-caspase-3 have been described [128], but not caspase-8. Antimicrotubule agents induce Bcl-2/Bcl-xL phosphorylation and an increase of Bax monodimer protein, which in turn, could be relocalized to mitochondrial membranes [129], and changed its permeability and facilitated cytochrome c release [130]. Other observations have recently indicated the existence of a molecular framework and cross talk between the endoplasmic reticulum (ER) and mitochondria in radiation-induced apoptosis [131], which can be interrupted by Bcl-2 protein at the level of the endoplasmic reticulum [132]. Bap31 complex is essentially localized in ER-membrane like intracellular death receptor (such as Fas/TNF receptor), which once activated could activate pro-caspase-8 [133], and initiate the apoptotic caspase cascade. Thus paclitaxel- and other antimicrotubule agents induced caspase-8 activation in a dependent and independent Fas/Fas-L ligation manner.

2.1.6.4 Role of Inhibitor of Apoptosis Protein (IAP) in the Apoptosis Induced by Taxanes

Preclinical studies of docetaxel mechanisms of action have already been investigated in different hormone-refractory or androgen-dependent and -independent prostate cancer cells [134]. Recently, it has been reported that docetaxel induced cell death during different apoptotic signal pathways in LNCap and PC-3 prostate cancer

cell lines [135]. An antiapoptotic gene, survivin, has also been implicated in prostate cancer. Surivin protein is a unique mammalian inhibitor of apoptosis protein [136], which has sequence similarities with other IAPs. Survivin is expressed only in the embryonic lung and other organs in developmental stages and is undetectable in normal adult tissues, other than the thymus and placenta. Nevertheless, survivin is also expressed in transformed cell types and in most human cancers. Suggesting that alterations in survivin gene regulation occur during tumorigenesis. Moreover, p34cdc2 kinase could phosphorylate this anti-apoptotic protein which is cell cycle-regulated [137]. In docetaxel-treated androgen independent PC-3 cells, an increased expression of survivin occurs within 4 hours after the beginning of the treatment. In contrast, no survivin induction was recorded in androgen responsive LNCaP treated cells, which instead expressed the putative apoptotic marker clusterin [138], whereas PC-3 cells did not.

Survivin is known to inhibit apoptosis by binding to the terminal effectors, caspase-3 and -7, but not to their corresponding pro-forms or the proximal initiator protease caspase-8 [136]. It has been implicated in preventing apoptosis and protecting cells from paclitaxel. LNCaP cells appeared to cleave caspase-3 and -7 in response to docetaxel treatment, whereas only 1 hour after treatment with 40 nM docetaxel, cleavage of caspase-8 was detected in PC-3 cells. No apical caspase-8 activity was detected in docetaxel-treated LNCaP cells. Androgen-independent PC-3 cells did not express the caspase-3-like effector protease, but appeared to use an entirely different apoptotic pathway by triggering the apoptosome caspase-9 activation through tBid-induced cytochrome c released from the mitochondria, by passing the caspase cascade. Phosphorylation of Bcl-2, release of cytochrome c from the mitochondria, cell shrinkage and nuclear DNA oligo-fragmentation are all induced by caspase-8 [139] without subsequent activation of caspase executors in these latter protastic cells. These findings concluded that the expression of survivin inhibits the activation of the terminal effector cell death proteases, caspase-3 and caspase-7, in PC-3 cell lines [135]. Thus, pathways for docetaxel-induced apoptosis support the evidence of different mechanisms of caspase activation and regulation, suggesting, that many other negative feed-back loops of caspase activation or activity may occur dependently of the cancer cell type. Further preclinical studies should be designed for the elucidation of the mechanism of caspase network regulation after taxanes treatment.

2.1.7 Cancer

Aberrant regulation of cell growth has traditionally been viewed as the major underlying mechanism for tumor formation; however, it is becoming increasingly clear that cellular changes that lead to inhibition of apoptosis play an essential role in tumor development [140]. It has been demonstrated that in neoplasias, cell cycle regulator genes/oncogenes such as *p53*, *ras* or *c-myc* suffer mutations, inactivation or deregulations associated to malignant transformation, these genes also regulate apoptosis in those cells [141]. Further genes, such as *bcl-2*, also over expressed in tumor cells, and the expression of *bcl-2* is currently considered a predictive factor for worse prognosis in prostate, breast and colon cancer and in neuroblastomas.

Many cancer chemotherapeutic drugs activate apoptotic mechanisms of tumor cell death, suggesting that factors that impair programmed cell death contribute to the resistance of tumor cells to cytotoxic drug treatment [142]. Elucidation of the apoptotic pathways that are triggered by anticancer therapies is thus an important area of study that may provide insights into the underlying causes of intrinsic and acquired drug resistance and facilitate the development of novel anticancer therapies.

2.1.8 Aim of the study

The aim of this study is to understand the molecular mechanism of Aven in taxane-induced apoptosis in human estrogen receptor (+/-) breast adenocarcinoma cell lines, MCF-7 and MDA-MB-231. For this purpose, firstly the dose kinetics of taxane-induced apoptosis was characterized and then Aven expression levels were checked in a time-dependent manner by western blot analysis. Since Bcl-xL has an established role in apoptosis, we studied the interaction of Aven with Bcl-xL. To further understand the role of Aven, cells were transfected by pSG-HA-Aven and also gene silencing technology was used. The effect of overexpression or downregulation of Aven in taxane induced apoptosis was investigated by using M30 Apoptosense ELISA test system. Therefore, this is the first study to our knowledge that shows the role of Aven in taxane induced apoptosis.

3 MATERIALS AND METHODS

3.1 Materials

3.1.1 Chemicals and Antibodies

Chemicals and antibodies that are used are listed in Appendix A.

3.1.2 Molecular biology kits

Molecular biology kits that are used for DNA isolation, apoptosis screening, plasmid isolation, siRNA treatment and RT-PCR are listed in Appendix B. Other specialty materials including DNA and protein markers are indicated in Appendix C.

3.1.3 Equipment

Equipment that are used for general laboratory procedures are listed in Appendix D.

3.1.4 Buffers and Solutions

Standard buffers and solutions used in cloning and molecular manipulations were prepared according to the protocols in *Molecular Cloning*: *A Laboratory Manual, Sambrook et al.,* 2001.

3.1.5 Buffer for agarose gel electrophoresis

1X TAE (Tris-EDTA-Acetate) buffer was used for preparation of 1% and 1.5% agarose gels. Gels are run at 80 V for 1 hour. DNA was visualized by including 0.005% ethidium bromide in the gel during its preparation.

3.1.6 Buffer for SDS polyacrylamide gel electrophoresis

1X Tris-Glycine-SDS (sodium dodecyl sulfate) buffer was used for polyacrylamide gel electrophoresis.

3.1.7 Primers and Plasmids

Aven primers were AF 5′-GATTTCAGTGTCCTCCTTAG-3′ and AR 5′-TTGCCATCATCAGTTCTC-3′. pSG5-Aven plasmid was provided kindly from John Hopkins University,USA.

Hs_Aven_3_Hp siRNA Sense r(CGAUAUCAAGAUAUUGAAA)dTdT
Antisense r(UUUCAAUAUCUUGAUAUCG)dAdT

3.2 Methods

3.2.1 Cell Culture

Human breast adenocarcinoma cell lines, MCF-7 and MDA-MB-231 cell lines , were cultured in RPMI-1640 containing filter-sterilized fetal bovine serum (10% FBS) and penicillin/ streptomycin (1% P/S 50 U/ml / 50 microgram/ml) plus additives L-glutamine in a humidified atmosphere with 5% CO_2 at 37 ^{o}C. Since L-glutamine is an unstable amino acid, medium was supplemented with L-glutamine just prior to use to a final concentration of 2 mM (0,292 g/L).

When cells were grown to confluency, they were detached with sterilized trypsin/EDTA solution. As the cells were detached in 37 ^{o}C incubator, trypsin activity was inhibited by the addition of complete medium. Cells were counted with a hematocytometer by the following formula:

$$\text{Cells/ml= average count per square X dilution factor X } 10^{12}$$

And equal volumes of cell suspension were seeded on to new dishes or flasks in appropriate densities.

3.2.2 Cryopreservation

To store cells for longer periods of times; cells were cryopreserved as follows: Cells were grown to late log phase, then trypsinized and spinned down at 300 g for 5 minutes. Cell pellet was resuspended in freezing medium (10% tissue culture grade sterile DMSO, as cryoprotective agent, in FBS). Cell suspension was transfered to cryovials, with each vial containing 10^6-10^7 cells/ml and then these cryovials were transfered to -80°C for storage.

When cryopreserved cells were needed, they were thawed rapidly and washed off residual DMSO with complete medium before seeded on to a 25 cm^2 flask.

3.2.3 Cell Treatments

Cells were grown to 90% confluency in 75 cm^2 flasks, trypsinized and seeded on six-well plate at a density of $5x10^5$ cells/per well or on 60 mm dishes at a density of $1x10^6$. Following day, cells were treated with Docetaxel (final 50 nM stock 12.4 μM) or Paclitaxel (final 50 nM stock 7.2 μM) in a time dependent manner for 1 hr, 2 hr, 4 hr, 8 hr and 12 hours. Total cell extraction was made for profiling Aven protein expression levels after these treatments.

For CoIP experiments, cells were treated with Docetaxel (50 nM stock 12.4 μM) or Paclitaxel (50 nM stock 7.2 μM) for 24 hours.

3.2.4 Total Protein Isolation

After cell treatments medium was removed, wells were washed once with ice-cold PBS, then 1 ml ice-cold PBS was added, cells were collected with a scraper and transfered to 1.5 ml eppendorf tubes. Cells were spinned down by cold centrifugation at 300 g for 5 minutes. Cell pellets were resuspended in 70 µl cold cell lysis buffer which is composed of 1% (v/v) Nonidet, 0.5% (w/v) sodium deoxycholate, 0.1% (w/v) SDS, 1 mM NaF, 1 mM Na_3VO_4, 0.1 mM PMSF and 1% (v/v) protein inhibitor coctail. After cell lysis, cell debris was removed by centrifugation for 10 minutes at 10,000 g and protein concentration was determined with Bradford assay.

For immunoprecipitation, protein isolation was made with 1% CHAPS buffer which is composed of 1% (w/v) CHAPS, 20 mM Tris-HCl (pH=7.5), 137 mM NaCl, 5 mM $MgCl_2$, 1mM EGTA, 1mM EDTA, 0.1 mM PMSF and 1% (v/v) protein inhibitor coctail.

3.2.5 Protein Concentration Determination

Protein concentration of total cell extracts were determined by Bradford method. The bovine serum albumin was used as standard. The BSA standards were prepared from 2 mg/ml stock solution of BSA as 0.2, 0.4, 0.6, 0.8 and 1 µg/µl of protein concentrations. 10 µl of these standard solutions were taken into 96-well plate, and for the unknown sample 1 µl was taken and diluted ten times with 9µl dH_2O. As a blank solution 10µl of dH_2O was put into the first two wells. 290 µl of (1:5) diluted Bradford reagent was added to all wells containing blank, standard and unknown samples. Absorbances were measured at 595 nm by a Bio-Rad microplate reader. The standard curve was plotted by using A_{595} values of BSA (y-axis) versus protein amounts of BSA (x-axis). The curve was linear with R^2-value (correlation coefficient) very close to 1. To determine protein concentration of unknown samples, A_{595} values were used by extrapolating them against the standard curve. For every assay, a new standard curve was plotted.

3.2.6 Immunoblotting

3.2.6.1 SDS-PAGE

Proteins were separated on a denaturing (SDS) discontinuous PAGE system. 30 μg total protein extracts were loaded to gels and gel preparation was as follows: Bio-Rad Mini Protean SDS-PAGE gel apparatus (for 1 mm gel) was assembled according to the manufacturer's instructions. First, 10% separating gel was poured; which contains, as the order of the addition of the solutions, 2.05 ml ddH_2O, 1.25 ml of 1.5 M Tris-HCl (pH=8.8), 25 μl of 20% (w/v) SDS, 1.65 ml of 30% /0.8% (w/v) acrylamide/bisacrylamide, 25 μl of 10% (w/v) APS and 5 μl TEMED. After polymerization of the first gel, 4% stacking gel was poured; which contains again with the order of addition, 1.54 ml ddH_2O, 0.625 ml of 0.5 M Tris-HCl (pH=6.8), 12.5 μl of 20% (w/v) SDS, 0.335 ml of 30% /0.8% (w/v) acrylamide/bisacrylamide, 12.5 μl of 10% (w/v) APS and 5 μl TEMED(these volumes are for one gel).Then the comb was inserted to form the wells in which protein samples were loaded.

Protein samples were prepared as follows: the volume that contains 30 μg of total protein extract was taken into eppendorf tubes and exactly the same volume of 2X Laemmli sample buffer (Sigma) was added and this mixture was boiled for 5 minutes at 95^0C. Then both protein marker (5-10 μL) and protein samples were loaded into the wells in 1X running buffer which was diluted from 10X running buffer that contains 30.3 g Tris-Base, 144.1 g Glycine and 10 g SDS in 1 liter dH_2O. The proteins were run through the stacking gel at 80 V for half an hour, and through the separating gel at 120V for an hour. After that, wet transfer was done as following.

3.2.6.2 Wet Transfer

Novex XCell II blotting apparatus was assembled as follows: PVDF membrane was soaked first with methanol for 30 sec, then rinsed with dH_2O and put into transfer buffer, which contains 1.45 g Tris base (final 12mM), 7.2 g glycine (final 96 mM), 200 ml methanol (final 20%) in 1 liter. Then SDS-polyacrylamide gel was taken out of the gel apparatus and put onto the pre-soaked Whatman filter paper. PVDF membrane was

placed on top of the gel, and finally another pre-soaked Whatman paper was put on the top of the membrane. Then this assembly was sandwiched between three pre-soaked blotting pads on both sides, which were altogether placed in the blotting module so that the gel was closest to the cathode plate(-). The module was put into the tank and fixed. The tank was filled with transfer buffer only half-way and the space between the two plates of the module was filled with transfer buffer all the way to the top. The tranfer was carried at 25 V for overnight in the cold room.

3.2.6.3 Antibody Incubations

After overnight transfer, PVDF membrane was taken out of the blotting module and put into blocking solution which was composed of 5%(w/v) non-fat dry milk and 0.2% Tween-20 in 1X PBS for 1-1.5 hour at room temperature. Then membrane was washed twice with PBS-T (0.2% Tween 20 in 1X PBS) for 15 minutes at room temperature. Membrane incubations with diluted primary antibodies were done for 2 hours at room temperature. The dilution solutions were prepared in 10 ml which contains 10% PBS-T, 10% milk diluent blocking solution plus 80% dH_20 plus 5 µl mouse monoclonal or rabbit polyclonal antibodies: anti-Aven (BD sciences), anti-Bcl-xL (Cell signaling,) , anti-HA (Abcam, 1mg/ml; final: 0,1 µg/ml), anti-β-actin (Abcam stock concentration unknown). After primary antibody incubation, membrane was washed three times with PBS-T for 15 minutes at room temperature. Then secondary antibody incubation was done for two hours at room temperature. Secondary antibody dilutions were 1/20000 for anti-mouse or anti-rabbit HRP conjugated antibody (Amersham). Then, membrane was washed three times with PBS-T for 15 minutes at room temperature. Last wash was made with 1XPBS for 5 minutes at room temperature.

3.2.6.4 Detection

Detection was done with enhanced chemiluminescence. Firstly, membrane was taken out and excess PBS was drained. Then freshly prepared detection reagent which was containing equal volumes of detection reagent 1 (stable peroxide solution) and detection reagent 2 (luminol/enhancer solution) was put on top of the membrane and

waited for 1 minute. As soon as possible, membrane was covered with plastic wrap on both sides. Covered membrane was placed in a film cassette, with the protein side facing up. In the dark room, a sensitive ECL film (Hyper-film ECL, Amersham) was positioned on top of the membrane and film was exposed for 30 seconds to the light emission. Then film was developed in developer solution and rinsed with dH_20. At the end, it was fixed in fixer solution and rinsed with tap water.

3.2.7 siRNA Treatment

Cells were seeded on six-well plate at a density of $2.5x10^5$ cells/per well. On the following day, siRNA treatment was done as follows: 5 nmol of Hs_Aven_3_Hp siRNA (19,23 µl) was mixed with serum free medium (80,77 µl). Then transfection reagent was added as 50 µl (1:10) for MCF-7 cells and 30 µl (1:6) for MDA-MB-231 cells and waited for 10 minutes at room temperature. Old medium was removed; 1900 µl fresh medium was added. Then prepared siRNA solution was added dropwise to the well and plate was swirled gently. After 24 hour incubation, protein and RNA isolations were made to check Aven down-regulation.

3.2.8 RNA Isolation with Trizol Method

After siRNA tretamnet, total RNA was extracted from each cell line using TRIZOL (Invitrogen). Firstly cell lines were washed with PBS twice than 500 µl TRIZOL added into 6 well plate. All cells were scraped and collected into a new tube. The cold chlorophorm (1:5 v:v) was added on to tube and waited on ice for 5 times. After centrifugation at 12000g for 15 min, the supernatant collected into a new tube without touching the middle white plaque. 500 µl ice cold isopropyl alcohol added and again mixed samples were centrifuged at the max speed for 5 min. Supernatant completely removed without touching the pellet and 500 µl ice cold ethanol added for washing process. All samples were gently washed with ethanol and then centrifuged at high speed for 5 min. Ethanol were gently removed and if it is required evaporation process applied using vacuum evaporator. The pellet was dissolved into 50 µl DEPC water. 2 µl RNA sample was dissolved in 98 µl DEPC water and 1:50 diluted samples

were spectrophotometrically calculated. The concentration of the RNA was quantified by determination of optical density at 260 nm (OD260).

3.2.9 One-Step RT- PCR

500 ng of total RNA was subjected to RT-PCR using One-step RT-PCR kit (Qiagen). The primers were forward 5′-GATTTCAGTGTCCTCCTTAG-3′ and reverse 5′-TTGCCATCATCAGTTCTC-3′ for Aven. RT-PCR was performed under the conditions as follows: reverse transcription at 50^0 C for 30 minutes, initial PCR activation step at 95^0C for 15 minutes, three-step cycling (denaturing at 94^0C for 30 s, annealing at 53^0C for 1 min, extension at 72^0C for 30 s) for 40 cycles and final extension at 72^0C for 10 min. The reactions were run, in parallel, for β-actin as endogenous control. PCR products were analyzed in 1.5% agarose gel with ethidium bromide.

3.2.10 Two step real time RT PCR

3.2.10.1 Reverse transcription assay (RT assay)

Reverse transcription (RT) was performed using a specific RT kit. The RT reaction mixture contained 1µl of total RNA, 500 ng of oligo (dT) primer, 5x RT reaction buffer, 10 mM dNTPs, and 200U of a reverse transcriptase (Qiagen) in a total volume of 20 µl. The all samples were incubated in 37°C for 1h. After incubation, 2µl cDNA product was dissolved in 98 µl DEPC water. The quantity of cDNA was calculated using spectrophotometer by determination of optical density at 260 nm (OD260). Purity was calculated using OD260/280 ratio.

3.2.10.2 Real time RT PCR

Real-time PCR was performed in 96-well 0.2 ml thinwall PCR plates using the iCycler Thermal Cycler (Bio-Rad) and carried out with QuantiTect SYBR Green PCR Master Mix (Qiagen), which contained HotStarTaq DNA Polymerase, QuantiTect SYBR Green PCR Buffer, and SYBR Green I. The real-time PCR reaction mixture contained 1x QuantiTect SYBR Green PCR Master Mix, 0.3 mM primer pairs, and

500 ng of cDNA in atotal volume of 25 µl. The mixture was heated initially at 95^0C. The mixture was heated initially at 95°C for 15 min in order to activate HotStarTaq DNA Polymerase and then followed by 40 cycles with denaturation at 94°C for 1min, annealing at 54 °C for 1min , and extension at 72 °C for 1 min.

3.2.10.3 Data expresion and analysis

Standard curves constructed from serial dilution of a known number of PCR product molecules were analyzed with the iCycler iQ Real-Time PCR Detection System (Bio-Rad). The standards were prepared using 100, 200, 300, 400 and 500ng control cDNA samples. Each assay for unknown samples was performed simultaneously with standard samples and negative control samples (non-RT samples) all in duplicate wells in the same plate. The baseline was set automatically by the software using data collected from cycles 2 to 10, and the threshold cycle (Ct) at which the amplification plot crossed the baseline was calculated. PCR efficiency was calculated automatically by the software using the following equation:

$$\text{PCR efficiency} = 10^{1/-\text{slope}} - 1$$

Quantification of the samples was accomplished from the Ct by interpolation from the standard curve to yield a copy number of each cDNA using a computer-assisted program. The raw abundance of Aven was divided β-actin values obtained from the same samples to derive a normalized value for each sample. In premilinary studies β-actin was constant in control and treated samples. Therefore β-actin mRNA used as internal standard. The relative difference between treatment conditions were calculated according following equations:

Fold change in target gene= copy number of experimental/copy number of control
Ratio experimental/control= fold change in target gene/fold change in reference gene

3.2.10.4 Melt curve analysis

Furthermore, the number of amplified products was identified by melt curve analysis. The melt curve protocols designed for increment temperatures of 0,5°C with a starting temperature of 54 °C and ending at 90 °C were repeated to ensure that primer dimers and other nonspecific products had been minimized or eliminated. As the melting temperature (Tm) was reached, the DNA denatured and released SYBR Green I, causing a sharp decline in fluorescence. This decrease in fluorescence was plotted as Fluorescence versus Temperature. Plotting the negative first derivative of these data versus the temperature change (dF/dT vs. Temperature) resulted in a melting peak and Tm for each amplified product.

3.2.11 Apoptosis and Cell Death

3.2.11.1 MTT Assay

Cells were grown to 90% confluency in 75 cm^2 flasks, trypsinized and seeded on 96 well plates at a density of $2x10^4$ cells/well in 100µl complete medium.On the following day, cells were treated with Docetaxel (50 nM stock 12.4 µl) or Paclitaxel (50 nM stock 7.2 µM) for 24 hours. After that, 10 µl of MTT labeling reagent from Roche (final concentration 0.5 mg/ml) was added to each well and incubated for 4 hours in humidified atmosphere (37 °C and 5% CO_2). To solubilize formazan dyes, 100 µl solubilization solution from Roche was added to each well and incubated for 12-16 hours at 37 °C and 5% CO_2. Absorbances of samples were measured spectrophotometrically at 550 nm by using ELISA microplate reader. As a reference filter, 655 nm was used according to the manufacturer's instructions. (Cell Proliferation Kit I Roche)

3.2.11.2 M-30 Apoptosense Assay

Cells were seeded on 96 well plates at a density of $1x10^4$ cells/well in 100 µl

complete medium. On the following day, cells were treated with Docetaxel (50 nM stock 12.4 μM), Paclitaxel (50 nM stock 7.2 μM), and Cisplatin (20 μM stock 3,3 μM) then incubated for 24 hours at 37^0C and 5% CO_2. After 24 hour drug treatment , 10 μl of 10% NP40 was added to each well and mixed onto a rotatory shaker for 5 minutes at room temperature. 2X25 μl of medium/lysate mixture was transfered to the wells of M-30 Apoptosense plate. Then assay was performed according to the manufacturer's protocol as follows: 75 μl of diluted HRP-conjugate solution was added to the each well containing cell lysates and it was agitated on a shaker for 4 hours at room temperature at 200 rpm. Then fluid was aspirated from the wells and washed five times with 250 μl wash solution. After washing step, 200 μl TMB substrate solution was added and plate was incubated for 20 minutes in darkness at room temperature. Then 50 μl of stop solution was added and mixed well. After 5 minutes incubation, spectrophotometric measurement at 450 nm was made.

Cells were pretreated with Aven siRNA, then drug application was done.

3.2.12 Immunoprecipitation

100-600 μg of total cell lysates were taken into 1.5 ml eppendorf tubes (see 'total protein extraction') and 1 μg of capture antibody (anti-HA rabbit polyclonal and anti-Bcl-xL mouse monoclonal) was added to cell lysates. Total volume was added up to 500 μl with total cell lysis buffer (cold). Then tubes were mixed on rocking platform for 1 hour at cold room. During this time, Protein G covalently coupled to sepharose beads were washed for equilibration. 300 μl of protein G sepharose suspension (50% slurry) was taken into eppendorf tube. Beads were washed with 1 ml cold lysis buffer (1% CHAPS) then centrifuged at 13200 rpm for 30 sec. at 4^0C. Supernatant was carefully removed without disturbing the bead pellet at the bottom. Washing was repeated once more, but this time supernatant was carefully removed with a flat gel-loading tip. Finally beads were resuspended in cold total cell lysis buffer so that beads and buffer together make up the same volume as in the first place.

After 1-hour incubation with capture antibody, equal volumes of washed protein G-sepharose (50% slurry) suspensions were added (50 μl) and tubes were mixed on rocking platform for another 2 hours at cold room. After that, sepharose beads, which

were bound to capture antibody plus bait protein, were collected with centrifugation at 13200 rpm for 30 sec. Supernatant was removed completely with flat gel-loading tips. Beads were washed six times with 1% CHAPS buffer (500 µl). Between each wash, tubes were centrifuged at 13200 rpm for 30 sec and supernatant was completely removed with flat gel-loading tips. After last wash, bead pellets were resuspended in 20-25 µl Laemmli sample buffer. Then they were boiled at 95^0C for 6 mins to dissociate complexes. Finally tubes were centrifuged at 13200 rpm for 1 min at 4^0C. Supernatants were loaded on 10% SDS-polyacrylamide gel, which was followed by immunoblotting as described above.

3.2.13 Transfection of MCF-7 Cells by Electroporation

Cells were grown to 75-80% confluency in 150 mm dishes.Then they wee trypsinized and spinned down at 300 g for 5 minutes. The cell pellet was resuspended in 1XPBS and cell number was counted. The volume that contains $4x10^6$ cells was taken and spinned down. The cell pellet was resuspended in 300 µl serum-free RPMI 1640 at room temperature. In an eppendorf tube, 10 ng plasmid DNA (pSG-HA-Aven) was taken and resuspended cell pellet was transfered to this tube. Cells and DNA were mixed by tapping gently.Then this mixture was put into the electroporation cuvette (4mm gap, BTX Cuvettes Plus). The cuvette was pulsed once with Electrocell Manipulator (ECM 630-BTX) with parameters set as 250 V, 725 Ω, 950 µF. Then 700 µl complete medium was added into the cuvette and 1 ml cell mixture was transfered to 60 mm dish, containing 2 ml complete medium. (RPMI-1640+ 10%FBS + 1% P/S) pSG-HA-Aven transfected cells were incubated in a 37^0C /5% CO_2 incubator for 24-48 hours before lysis for total protein extraction.

3.2.14 Transformation

7 ng DNA or whole ligation mixture (pSG-HA-Aven , pSG) was added onto ice-thawed 250 µl competent E.coli strain (DH5-α) on ice and waited for 20 minutes on ice. After this incubation, cells were heat-shocked at 42^0C for 90 seconds.Then tube was put back on ice for one minute. 500 µl pre-warmed LB (liquid) broth without any antibiotic

was added and cells were recovered for 45 minutes at 37^0C with shaking. Then whole tube was spread on selective LB agar medium containing antibiotic ampicillin (conc.100 μg/ml). Plates were incubated overnight at 37^0C for colony formation.

3.2.15 Midi-Preparation of Plasmid DNA and Restriction Endonuclease Digestion

2 ml LB Broth containing antibiotic ampicillin (100 μg/ml) was inoculated with a single transformant colony. After growth at 37^0C for 8 hours with vigorous shaking (250-270 rpm), 1/500 of this culture was inoculated into a larger culture (50 ml) and continued to grow for 12-16 hours at 37^0C with vigorous shaking.

Then plasmid DNA was prepared according to the manufacturer's instructions (QIAGEN Plasmid Midi Kit 100 Purification Handbook). The quality and quantity/concentration of the plasmid DNA were checked by agarose gel electrophoresis (1% agarose gel 1X TAE) and spectrophotometer (absorbance at 260 nm with A_{260}/A_{280} ratio close to 1.8)

For further confirmation of the plasmid DNA identification and for preparation of mock plasmid, restriction endonuclease digestions were performed in 37^0C waterbath for 2-6 hours with the following enzymes; BamHI, XbaI , EcoRI; according to the manufacturer's instructions (Promega). Digested DNA fragments were run on an 1% agarose gel with 1 kb DNA marker.

To generate mock plasmid, pSG-HA-Aven plasmid was cut with XbaI and BamHI for 6 hours in 37^0C water bath. Then digested DNA was treated with Klenow Fragment for 10 minutes at 37^0C and run on the 1% agarose gel.The band around 4 kb was excised and gel purified with QIAGEN Gel Extraction Kit according to the manufacturer's instructions. After gel purification of DNA fragment, it was run on the gel to check for quantity. The ligation reaction was performed for 16 hours at 15^0C .Then re-ligated plasmid was transformed to competent cells (DH5α) and plasmid DNA is prepared with midi-prep as mentioned before.

3.2.16 Statistical Analysis

The results are expressed as mean ± SEM and the mean values were compared using Students t-tail test Value of $P< 0.05$ is considered statistically significant.

4 RESULTS

4.1 MTT Assay

The sensitivity of human adenocarcinoma cell lines (MCF-7 and MDA-MB-231) to paclitaxel and docetaxel was investigated by MTT assay. The cells were treated for 24 hours in a medium containing varying concentrations of paclitaxel (1-50 nM) or docetaxel (1-50 nM). Both drugs were induced dose-dependent reduction in cell growth. 50nM Paclitaxel treatment for 24h inhibited growth of MCF-7 by 58% and MDA-MB-231 by 44%. For docetaxel, 50 nM drug concentrations caused growth inhibition by 55% and 70% for 24h in MCF-7 and MDA-MB-231 cell lines respectively. MDA-MB-231 cells showed higher sensitivity compare to the MCF-7 for paclitaxel, the decreament was by 43.55% in cell viability at 50 nM concentration (p=0,026) whereas MCF-7 cells showed higher sensitivity for docetaxel with 55.83% decrease in cell viability at 50 nM concentration (p=0,027). Based on these results, 50 nM drug concentrations were used for further experiments. (Figure 4.1 and 4.2.)

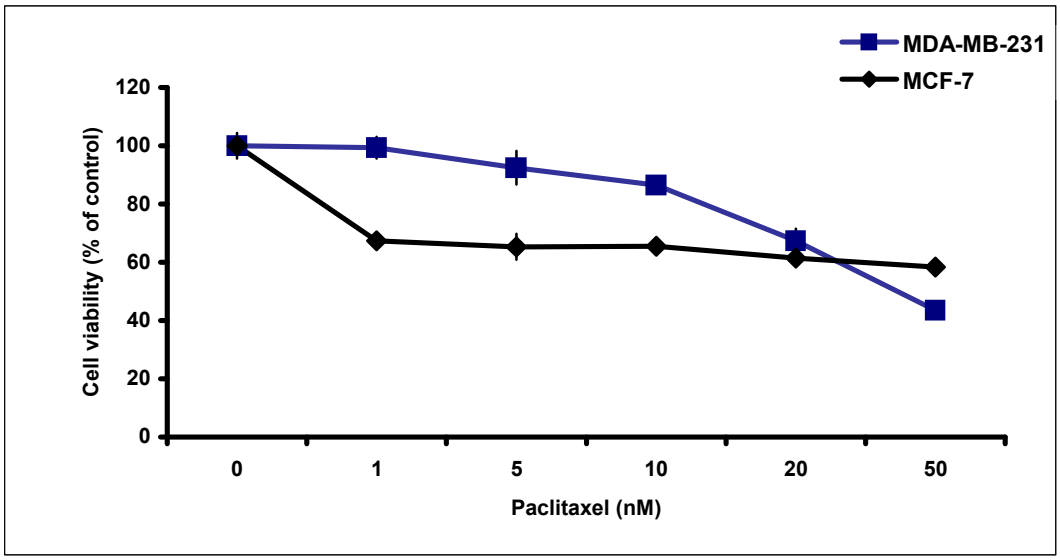

Figure 4. 1 Paclitaxel induced cytotoxicity in MDA-MB-231 and MCF-7 cells. Cells in 96- well plates were treated with indicated concentrations of Paclitaxel for 24 hours. Cell viabilities were assessed by MTT assay. Data are shown as mean ± SEM % of untreated control and representative of two independent experiments in duplicate. P<0,05

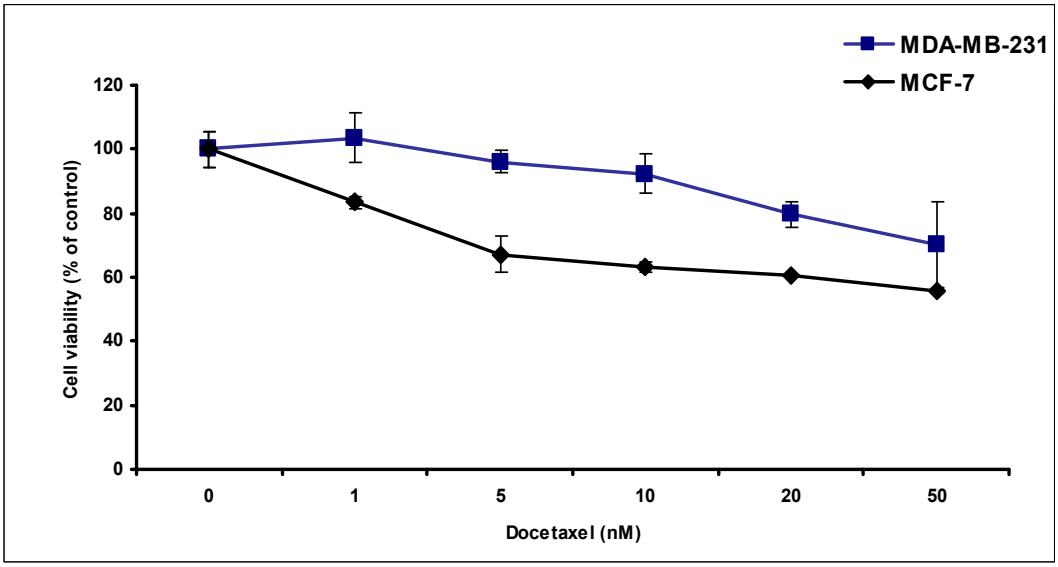

Figure 4. 2 Docetaxel induced cytotoxicity in MDA-MB-231 and MCF-7 cells. Cells in 96 well plates were treated with indicated concentrations of Docetaxel for 24 hours. Cell viabilities were assessed by MTT assay. Data are shown as mean ± SEM % of untreated control and representative of two independent experiments in duplicate. P<0,05

4.2 Expression and modulation of Aven by TaxaneTreatment

In order to answer the role of Aven in taxane induced apoptosis, endogeneous Aven protein levels were determined in untreated and docetaxel or paclitaxel treated MCF-7 and MDA-MB-231 cells by immunoblotting assay. Paclitaxel and docetaxel treatments were done in a time dependent manner, starting from 1 hour up to 12 hours at 50nM final concentration. We immunoblotted total protein extracts with anti-Aven antibody(at 1/5000 dilution 0,83 μg/ml concentration). These immunoblotting experiments demonstrate that the intensity of Aven protein bands did not change with drug treatment in either cell line. We conclude that Aven protein levels are unchanged with paclitaxel or docetaxel treatment in both MCF-7 and MDA-MB-231 cell lines (Figure 4.3 and 4.4). Equal protein loading was confirmed by immunoblotting the same membrane with an anti-β-actin antibody at 1:5000 dilutions.

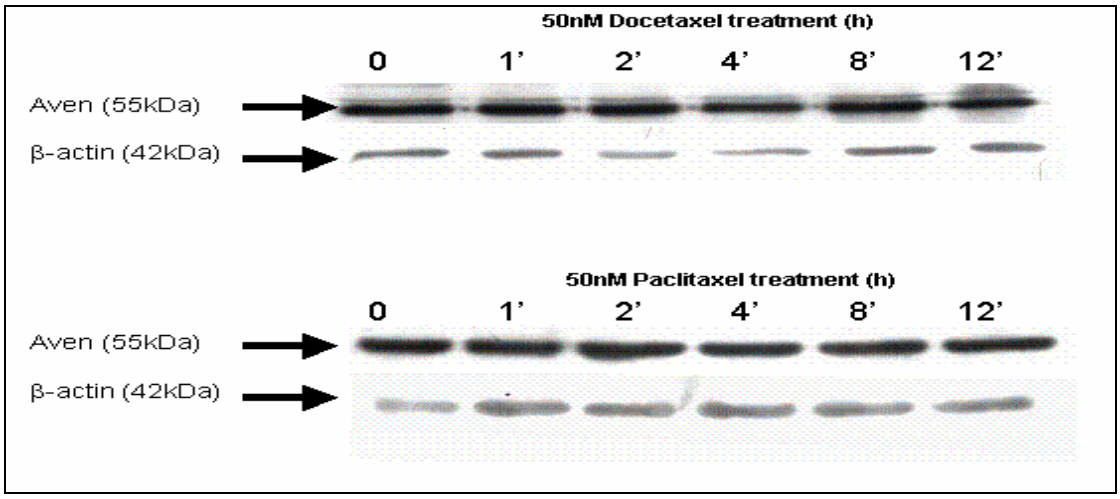

Figure 4. 3 Taxane-induced regulation of Aven in MDA-MB-231 cells. MDA-MB-231 cells were grown on 6-well plates ($5x10^5$ cells/well) and treated with 50 nM Docetaxel or 50 nM Paclitaxel for 0-12 h. Total protein lysates were isolated and Aven levels were detected by immunoblot analysis using specific antibody.β-actin was probed as a loading control for immunoblots and results are representative of three independent experiments.

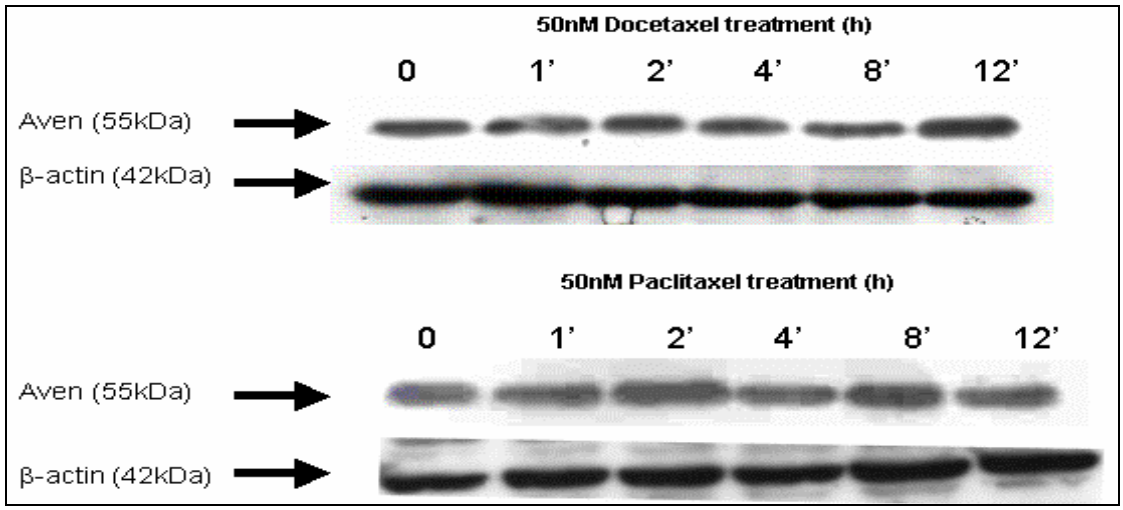

Figure 4. 4 Taxane-induced regulation of Aven in MCF-7 cells. MCF-7 cells were grown on 6-well plates (5x105 cells/well) and treated with 50 nM Docetaxel for 0-12 h.Total protein lysates were isolated and Aven levels were detected by immunoblot analysis using specific antibody. β -actin was probed as a loading control for immunoblots and results were representative of three independent experiments.

4.3 Modulation of Aven-Bcl-xL interaction by Taxane Treatment

The endogenous Aven (top row) and Bcl-xL (middle row) levels in total cell lysates were examined by western blotting after 24-hour drug treatment in both cell lines. The protein-protein interaction of Aven with Bcl-xL was analyzed by co-immunoprecipitation assays. After 24 hours of taxane treatment of both MCF-7 and MDA-MB-231 cell lines, endogeneous Bcl-xL was immunoprecipitated out of the total protein extracts by using 1 μg of anti-Bcl-xL antibody (rabbit polyclonal IgG1). Immunocomplexes formed were dissociated by boiling in Laemmli sample buffer at 95^0C and were resolved on a 10% SDS-polyacrylamide gel. The presences of Aven in Bcl-xL immunoprecipitates were examined by western blotting with anti-Aven antibody (bottom row). Subsequent analysis with the anti-Aven antibody (monoclonal mouse) demonstrated that the bait Bcl-xL protein was able to precipitate endogenous Aven. Comparison of lane 1 and lane 2 or lane 1 and lane 3 in Bcl-xl immunoprecipitates blotted by anti-Aven antibody demonstrate that docetaxel or paclitaxel treatment does not affect the association of Bcl-xl with Aven. These experiments were repeated 3 times and similar band intensities were observed in untreated and treated lanes in all experiments (Figure 4.5).

Note that docetaxel and paclitaxel treatment results in phosphorylation of Bcl-xl (middle row, second and third lanes). This is demonstrated by the appearance of a slow mobility band in Bcl-xl immunoblots specifically in treated cells. This effect was observered in both MCF-7 and MDA-MB-231 cell lines (Figure 4.5).

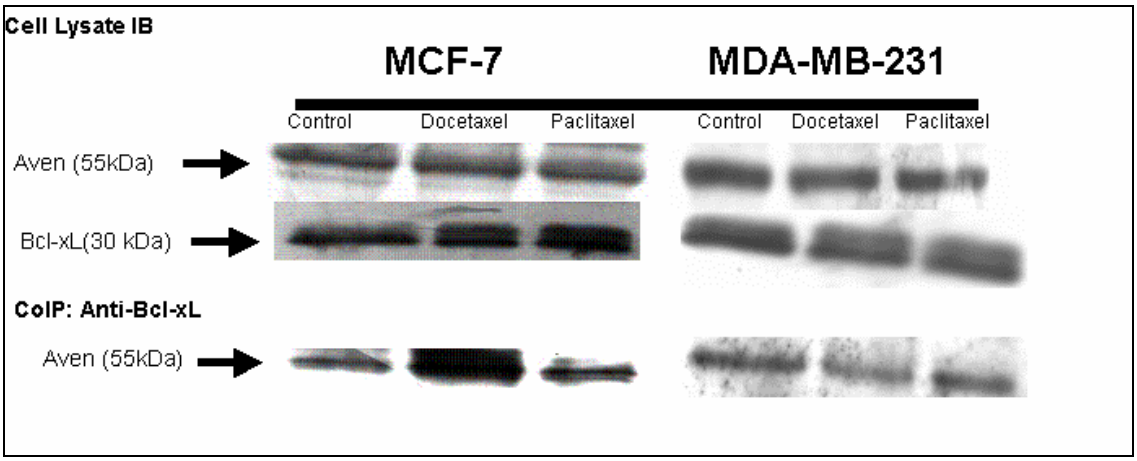

Figure 4. 5 Taxane-induced regulation of Aven-Bcl-xL interaction. MCF-7 and MDA-MB-231 cells were grown on 6-well plates (5x105 cells/well) and treated with 50 nM Docetaxel or Paclitaxel for 24 h. Total cell lysates and Bcl-xL immunoprecipitates were separated by SDS-PAGE and immunoblotted with the indicated antibodies. Results were representative of three independent experiments.

4.4 Overexpression of Aven

Both cell lines were transfected with pSG-HA-Aven and mock plasmid* to check whether overexpression of Aven may have a role in drug resistance. Cell lysates were subjected to western blotting with anti-HA antibody to reveal transfected HA-tagged Aven proteins (top lanes) and also subjected to immunoprecipitation with HA-antibody followed by anti-Aven immunoblotting (bottom lanes).

Immunoblotting results showed that the amount of Aven protein in transfected cells was dramatically increased. The applicability of anti-HA rabbit polyclonal antibody for immunoprecipitation assay and as a control for co-IP assay, HA-Aven was immunoprecipitated with anti-HA antibody and immunoblotted with anti-Aven mouse monoclonal antibody. (Figure 4.6.) However, mock-transfected cell extracts showed that endogenous Aven was also immunoprecipitating with anti-HA antibody. Note that HA immunoprecipitates of untransfected cells blotted by Aven antibody reveal the presence of nonspecific association of Aven protein with HA-antibody. However the amount of Aven immunoprecipitated from transfected samples was dramatically larger than this non-specific band (compare lane 1 to lane 2 Figure 4.6)

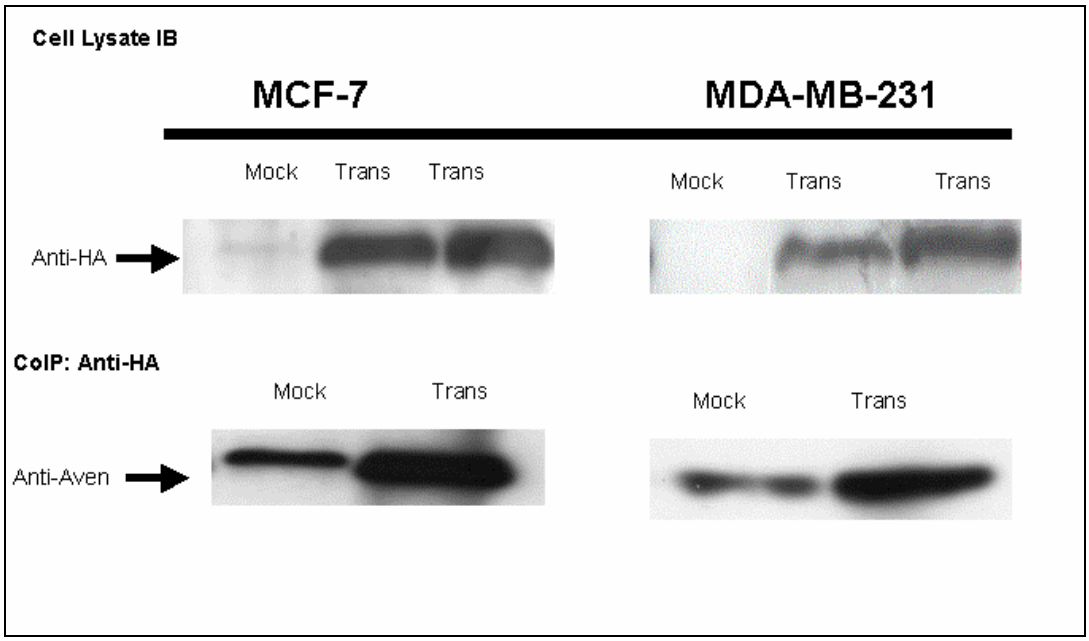

Figure 4. 6 Aven overexpression in MCF-7 and MDA-MB-231 cells.Cells were transfected with HA-Aven or mock plasmid.Total cell lysates and anti-HA immunoprecipitates were separated by SDS-PAGE and immunoblotted with indicated antibodies.

∗ Plasmid DNAs to be transfected (pSG-HA-Aven and mock plasmid pSG) were midi-prepared and checked by agarose gel electrophoresis and spectrophotometry. Diagnostic restriction endonuclease digestion were performed beforehand for confirmation of the identities of the vector (data not shown)

4.5 Downregulation of Aven with siRNA treatment

The silencing of Aven gene with siRNA was performed to understand whether siRNA treatment together with taxanes sensitizes cells or not. Therefore both MCF-7 and MDA-MB-231 cell lines were transfected with 5 nmol of Hs_Aven_3 HP (Qiagen) with siRNA transfection reagent. Downregulation of Aven mRNA was determined by both one-step RT-PCR and quantitative real time PCR. One-step RT-PCR was performed with a suitable commercial kit (Qiagen) and then products were run on 1.5% agarose gel with ethidium bromide. β-actin primers were used as an endogenous control. The band intensities of the siRNA treated samples were decreased dramatically compare to the control (Figure 4.7). The effective concentration of Aven siRNA was determined as 1:6 (5nmol siRNA:30µl hyperfection reagent) for MDA-MB-231 cell

lines . This ratio was 1:10 (5nmol siRNA:50µl hyperfection reagent) for MCF-7 cell lines.

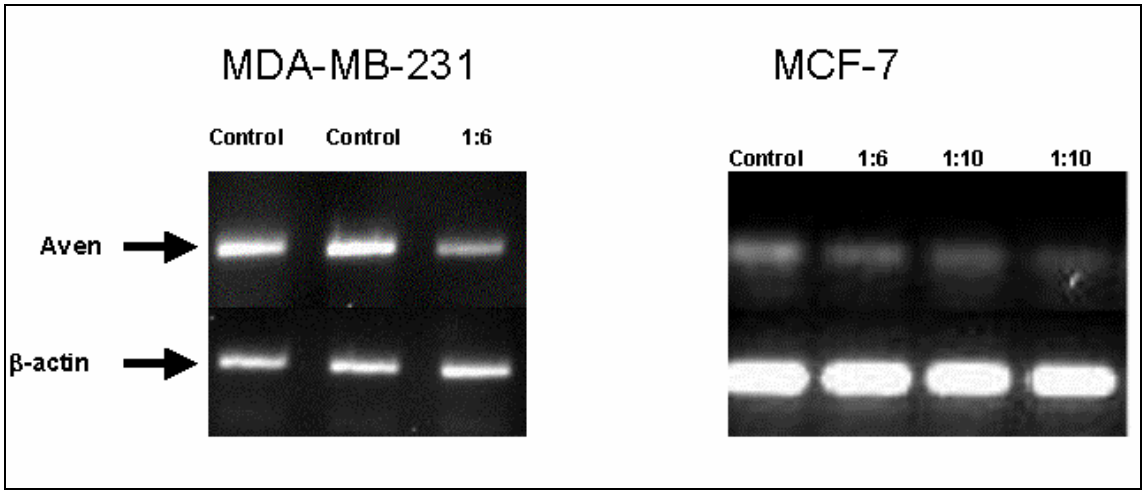

Figure 4. 7 One step RT PCR results. MDA-MB-231 cells were grown on 6-well plates (2.5x10^5 cells/well) and transfected with 5 nmol (Hs_Aven_3 HP). After 24 hours, total RNA was isolated with Trizol method and it was subjected to RT-PCR using One-step RT-PCR kit (Qiagen). PCR products were analyzed in 1.5% agarose gel with ethidium bromide. β-actin was used as an endogenous control.

The real time RT-PCR was performed to quantify Aven mRNA downregulation. Total RNA was converted to cDNA by reverse transcription, and then 500 ng cDNA was PCR amplified with QuantiTect SYBR Green PCR Master Mix (Qiagen) by using iCycler Thermal Cycler (Bio-Rad). The standard curve was contructed from known amounts of control sample, quantification of unknown samples were made by extrapolating Ct values to standard curve. For normalization, copy number was divided by β-actin values of the same sample, since β-actin values were not changing upon treatment. Relative Aven mRNA/b-actin was plotted. The Aven siRNA treatment caused 2.3 and 1.7 fold decrement in intracellular Aven mRNA level in MCF-7 and MDA-MB-231, respectively. (p=0.003)

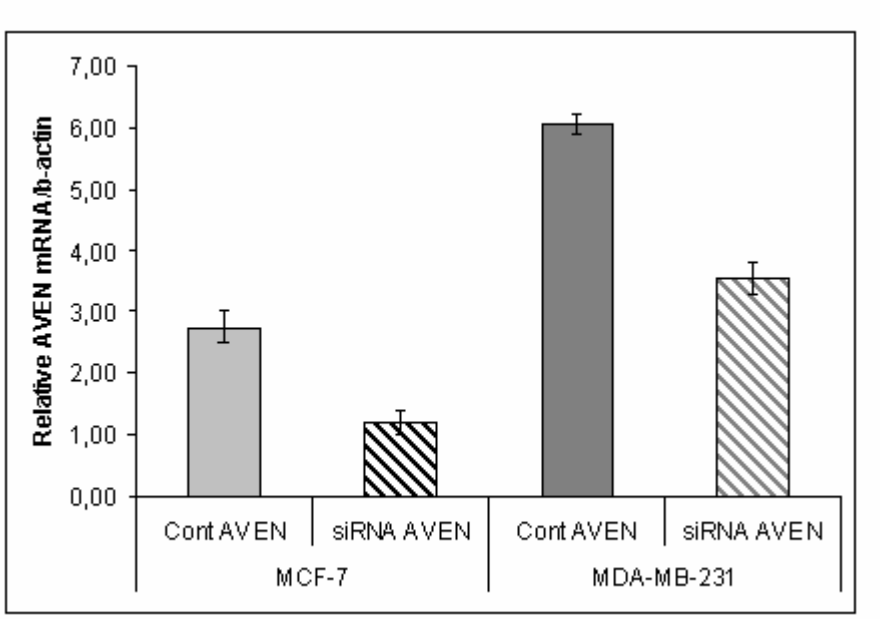

Figure 4. 8 Quantitative real-time RT-PCR results. Aven copy number for control and siRNA transfected samples were calculated by using standard curve. These values were normalized by dividing with β-actin values. The relative values for control and siRNA transfected samples were plotted. The data were expressed as mean± std and representative of two experiments in duplicate. P<0,005

The inhibitory effect of siRNA on Aven expression was determined by western blotting on the protein level. After 24 hour of posttransfection, endogeneous Aven levels were determined in untreated and siRNA tranfected cells with immunoblotting. Total protein lysates were imnmunoblotted with specific anti-Aven antibody (at 1/5000 dilution 0,83 μg/ml concentration). Immunoblotting results demonstrated that Aven expression level decreased upon siRNA treatment. Although lower concentration ratio of hyperfection reagent usage in MDA-MB-231 cells, the downregulation of Aven protein was more efficient then MCF-7 cells.

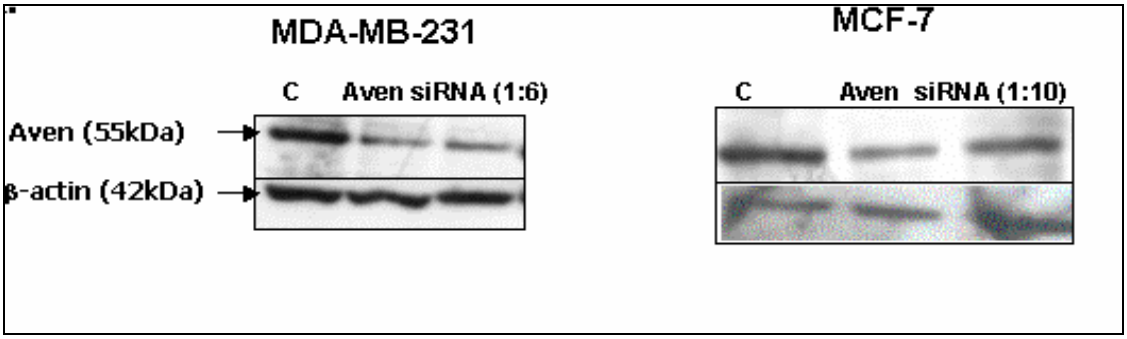

Figure 4. 9 Western blot results for siRNA treatment. Cells were transfected with Hs_Aven_3 HP siRNA.Total cell lysates were separated by SDS-PAGE and immunoblotted with indicated antibodies.

4.5 M-30 Assay

The role of Aven overexpression and downregulation in taxane induced cell death were determined with M30 Apoptosense assay. During apoptosis, caspases cleave various cellular proteins. In epithelial cells, one of those substrates is the intermediate filament protein cytokeratin 18 (CK18). Cleavage of CK18 results in a collapse of the keratin filaments into large aggregates. The M30 antibody recognizes a neo-epitope which is exposed after cleavage of CK18 by caspases after the aspartic acid residue 396 (CK18Asp396).[159] Cleavage at this site occurs early during apoptosis and is mediated by caspase-9 as well as caspase-3 and caspase-7.[168] Cells were both transfected with pSG-HA-Aven plasmid or with Hs_Aven_3 HP siRNA for 24 hours, and then treated with taxanes for another 24 hours. Cells were also treated with 20 μM cisplatin as apoptosis positive control. Samples were reacted with the mouse monoclonal antibody ″M5″ directed against CK18, which has been immobilized to the polystyrene wells and, simultaneously, with the HRP- (Horseradish peroxidase) conjugated M30 monoclonal antibody directed against the CK18Asp396 neo-epitope. Following the formation of the

solid phase/antigen/labeled antibody sandwich, excess unbound conjugate was removed by a washing step. TMB substrate was added and color developed in proportion to the bound analyte. The color development was then stopped and color intensity was measured in a microplate reader at 450 nm. By plotting a standard curve from known concentrations versus measured absorbance, the amount of antigen in the same sample was calculated. The concentration of the M30-antigen was expressed as Units per Liter (U/L).

The apoptotic cell death in MCF-7 cells was shown as absorbance at 450 nm and then the antigen amount was calculated from the standard curve. In non-transfected MCF-7 cells, the M30 antigen levels increased by 1.6 fold after taxane treatment. This increment was 2.2 fold due to cisplatin treatment. When MCF-7 cells overexpressed Aven, the increment of M30-antigen was 2 fold after taxanes treatment. Thus overexpression caused more apoptotic cell death for taxanes. Whereas downregulation of Aven caused only 1.2 fold increment in M30 levels after taxane treatment. Moreover, cisplatin had less toxic effect on MCF-7 cells when Aven was overexpressed since M30 levels increased by 1.5 fold compare to the control. Whereas downregulation of Aven seemed to be sensitizing the cells for cisplatin and causing more apoptotic cell death since there was 2.5 fold increament in M30 antigen levels. (Figure 4.10 p=0,049 and 4.11).

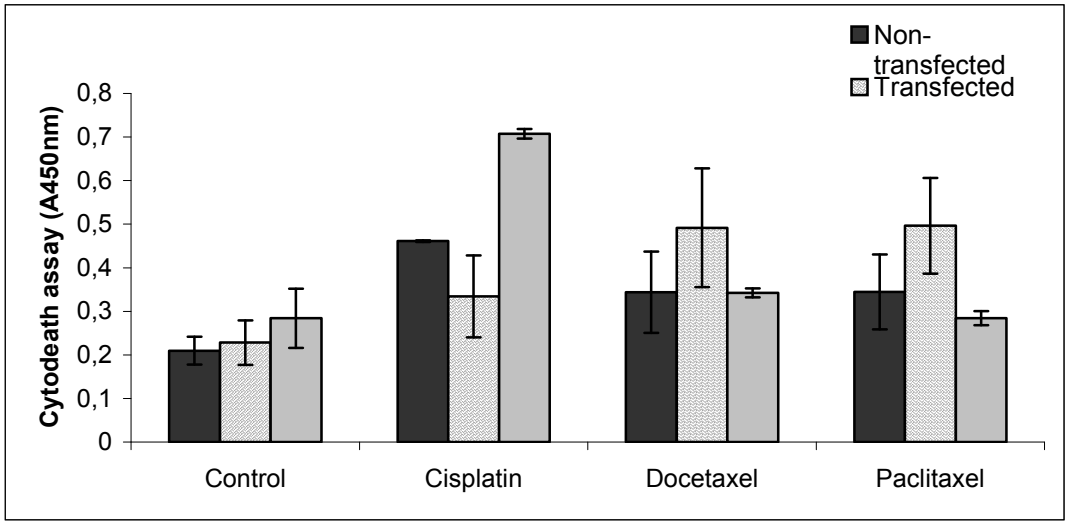

Figure 4. 10 M30 Apoptosense ELISA Assay for MCF-7 cells. Cells were grown on 96-well plate ($1x10^4$ cells/well). They were transfected with pSG-HA-Aven or Hs_Aven_3 HP siRNA. 24 hour of posttransfection, they were treated with Docetaxel (50 nM) or Paclitaxel (50 nM) or Cisplatin (20 μM). Apoptotic cell death was determined with M-30 apoptosense assay. Data were expressed as mean±SEM representative of two experiments. P<0,05

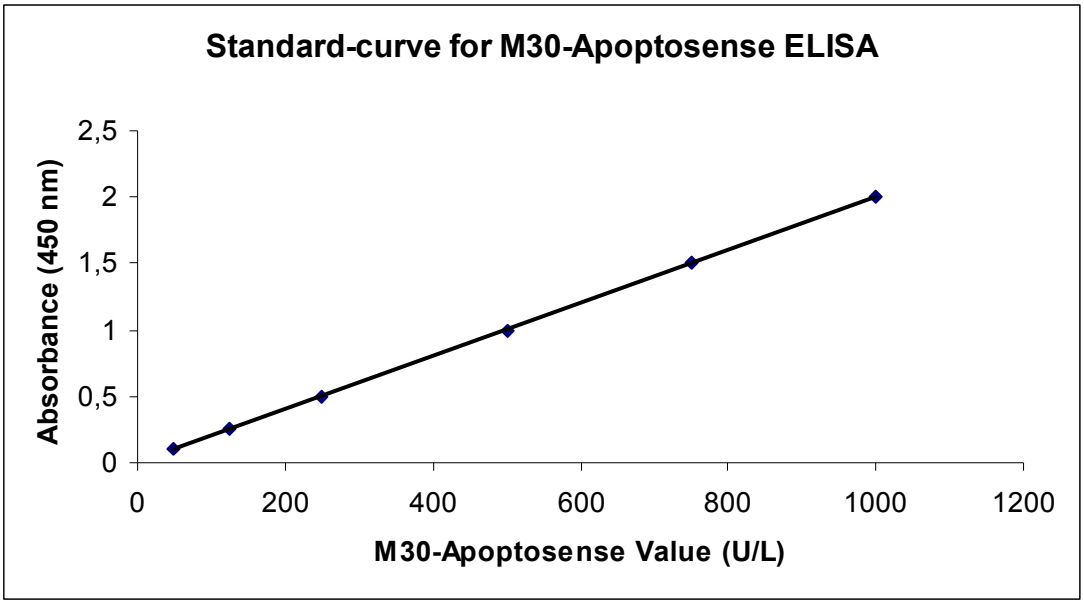

Figure 4. 11 Standard curve for M30-Apoptosense ELISA, lot PE0024

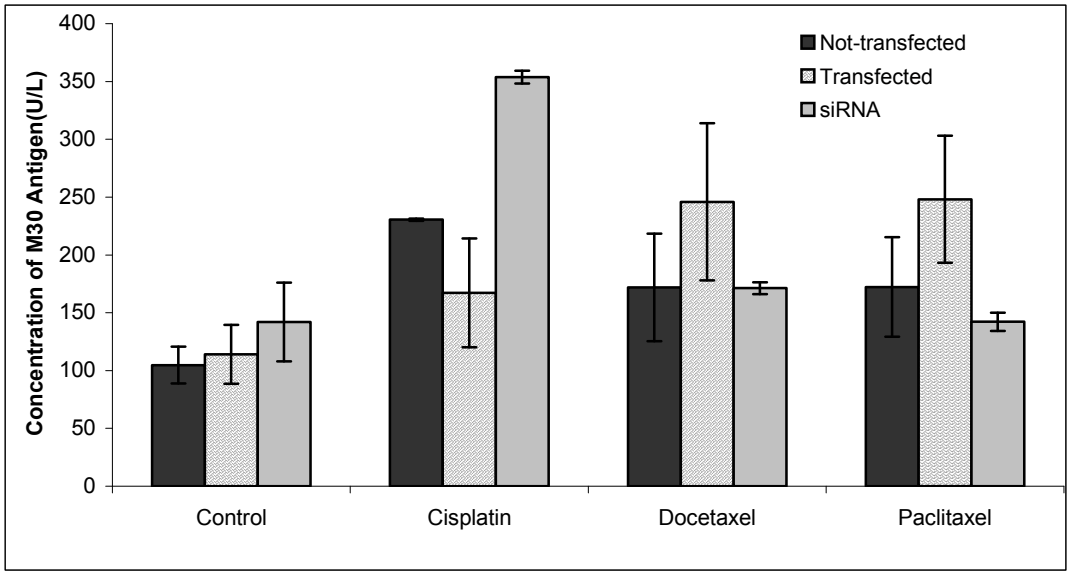

Figure 4. 12 The concentration of M30-antigen for MCF-7 cells as Units per liter (U/L). Standard curve

In MDA-MB-231 cells, M30 antigen levels were increased by 3.1 and 2.8 fold after docetaxel and paclitaxel treatment. For cisplatin this increment was 3.3 fold. Aven overexpression in MDA-MB-231 cells sensitized cells against taxane induced apoptosis and also cisplatin-induced apoptosis. (Figure 4.13 p=0,027) The M30 antigen levels

were increased by 3.4 and 3.1 fold upon paclitaxel an docetaxel treatment, for cisplatin it was 3.9 fold.(Figure 4.14 p=0,02) But sensitization was not that much high for MDA-MB-231 cells when docetaxel transfected and not-transfected cells were compared. In contrast, downregulation of Aven caused a decrease in apoptotic cell death. (Figure 4.13.) The fold change in M30 antigen levels was 1.3 and 1.2 for docetaxel and paclitaxel respectively. For cisplatin the fold change was 1.4. Thus downregulation caused less apoptotic cell death. (Figure 4.14)

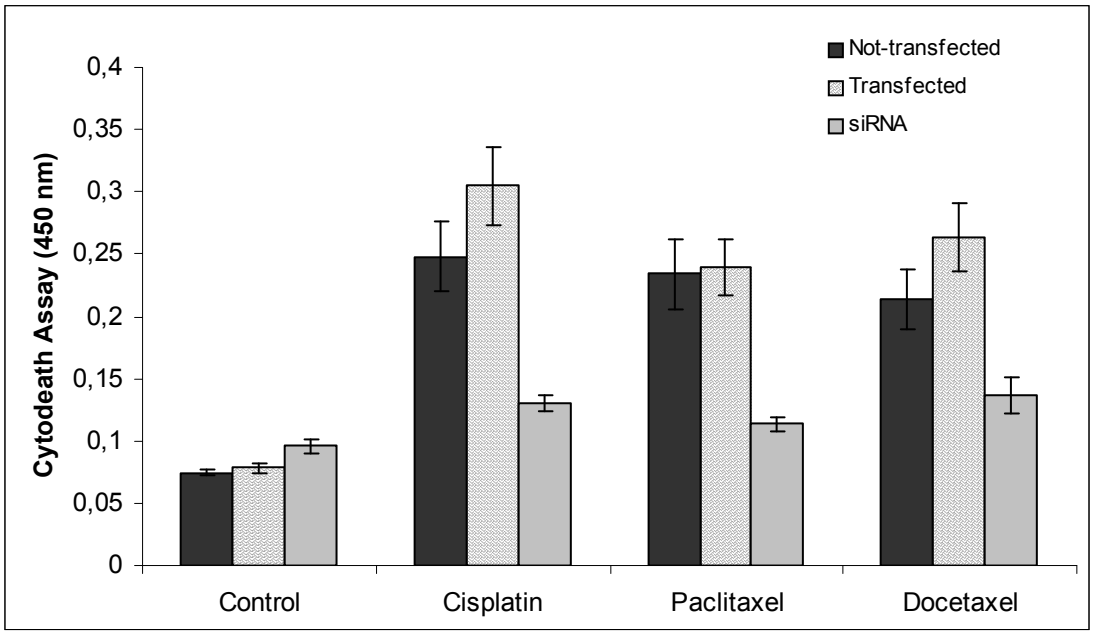

Figure 4. 13 M30 Apoptosense ELISA assay for MDA-MB-231 cells. Cells were grown on 96-well plate ($1x10^4$ cells/well). Cells were transfected with pSG-HA-Aven or Hs_Aven_3 HP siRNA. 24 hour of posttransfection, they were treated with Docetaxel (50 nM) or Paclitaxel (50 nM) or Cisplatin (20 μM). Apoptotic cell death was determined with M-30 apoptosense assay. Data were expressed as mean±SEM representative of two experiments. P<0,05

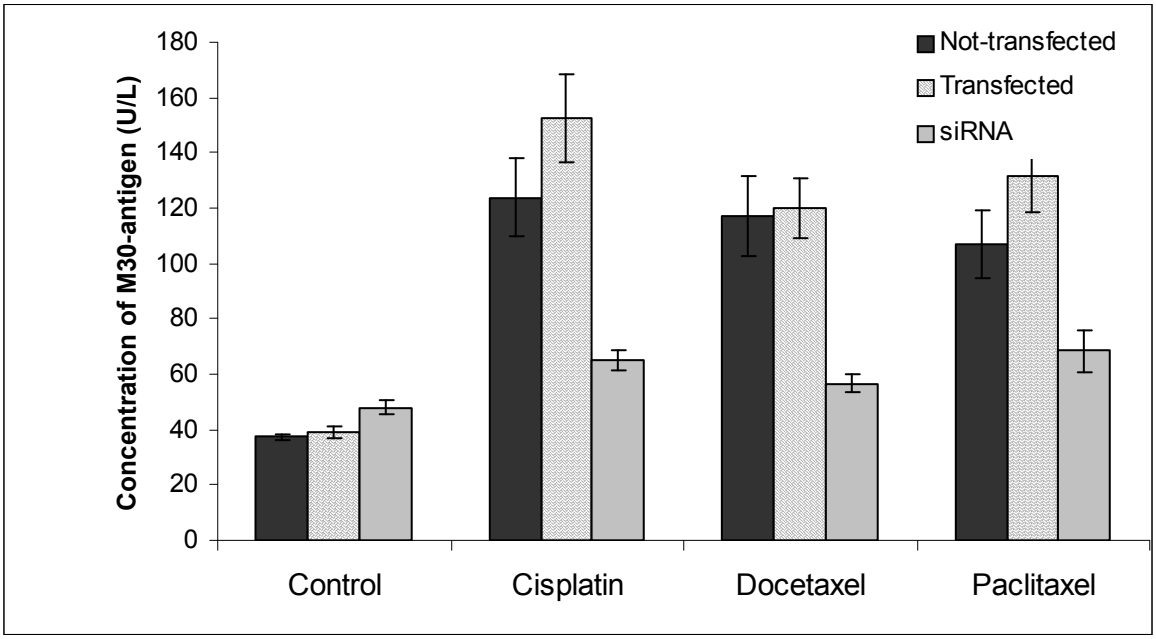

Figure 4. 14 The concentration of M30-antigen for MDA-MB-231 cells. Units per Liter (U/L).

5. DISCUSSION

Taxanes are one of the most powerful classes of novel antitumor agents and has become an integral part of several commonly used chemotherapy regimens in metastatic breast cancer treatment. They are natural products that act by inducing microtubule stabilization, disruption of the mitotic spindle apparatus, and dysregulation of mitotic events [2]. Thus, stabilization of the spindles inhibits cellular trafficking, which probably restricts DNA repair mechanism, and therefore forcing cells to the commitment of programmed cell death [3,100]. Apoptosis induced by taxane is a complex process associated with various signal transduction pathways (as illustrated in Fig 2.6). They induce hyperphosphorylation of Bcl-2/Bcl-xL which abolish their anti-apoptotic function during mitotic arrest [8-10] or they cause upregulation of pro-apoptotic Bax protein [9,106]. Therefore regulation of gene expression and modulation of proteins have an important role during taxane-induced apoptosis.

Aven is a novel apoptosis inhibitor, which binds to both Bcl-xL and Apaf-1 [20]. Identified in yeast two-hybrid, Aven expression was detected in many tissues such as heart, skeletal muscle, kidney, liver, pancreas and testis. Aven homologs are also found in other species and human genome sequencing places Aven on chromosome 15. Bcl-xL is an anti-apoptotic protein and it forms heterodimers with Bcl-2 family members Bax and Bak, and inhibits the proapoptotic activities of these proteins [169,170]. Bcl-xL interaction with Aven has been shown to enhance cell survival [20,21]. Apaf-1 is the mammalian homolog of *Caenorhabditis elegans* CED-4; it hydrolyzes dATP and interacts with the released cytochrome c leading to the formation of an oligomeric multiprotein complex, the apoptosome. Oligomerization of Apaf-1 and recruitment of caspase-9 leads to activation of caspase-9 [37,38]. Aven interaction with Apaf-1 inhibits self-association of Apaf-1 and impairs caspase-9 activation [20]. Suppression of Apaf-1 mediated cell death and involvement of Aven in cell survival by interacting with Bcl-xL makes this protein a possible candidate for our study. Therefore

it was the interest to study the role of Aven in taxane induced apoptosis.

Here we show that increasing concentration of docetaxel and paclitaxel decreases cell viability in dose-dependent manner in both cell lines. The cell viability decrement was by 43.5 % and 58.3 % for MDA-MB-231 and MCF-7 cells for paclitaxel treatment. The paclitaxel treatment has more inhibitory effect on MDA-MB-231 cell line. Whereas for MCF-7 cells docetaxel treatment was more effective than paclitaxel. MCF-7 cells are moderately differentiated, estrogen receptor-positive, non-metastatic mammary-infiltrating ductal adenocarcinoma cells [152] and MDA-MB-231 cells are poorly differentiated, estrogen receptor-negative, highly metastatic mammary adenocarcinoma cells [153]. The difference in the effectiveness of these drugs on these cell lines could be explained by the presence of estrogen receptor and metastatic behaviour.

After characterization of kinetics in taxanes-induced apoptosis, the role of Aven in taxane-induced apoptosis was investigated. Total protein extracts after 0-12 hour treatments were isolated and Aven levels were checked by immunoblotting. The results show that Aven expression levels do not change with taxane treatment. According to immunoblotting results, Aven expression is not regulated by taxanes. However, this does not show that Aven protein has no role in taxanes-induced apoptosis.

Chaou et al (2000) showed that Aven binds the anti-apoptotic mammalian and viral Bcl-2 proteins, but not the pro-apoptotic family members [20]. Aven also fails to bind to the pro-apoptotic caspase cleavage product of Bcl-xL (ΔN61) [20]. The BH1 domain of Bcl-xL is also involved in Aven binding. Mutations in BH1 (mt7) that inactivate the antiapoptotic function of Bcl-xL abolished binding to Aven [20]. In contrast, a BH1 mutant of Bcl-xL (Bcl-xL mt1) that retains its antiapoptotic function but loses its ability to heterodimerize with Bax and Bak also retains its ability to bind Aven [20]. Only those mutants of Bcl-xL that bind Aven also retain their antiapoptotic activity. Bcl-xL phosphorylation upon taxane treatment has been shown and has resulted in inactivation of Bcl-xL which sensitizes cells for apoptosis [60]. In this study for further characterization, Aven interaction with Bcl-xL was checked after 24-hour drug treatment. For immunoprecipitation, amount and volume of the total protein extract to start with, amounts of the capture antibodies and protein G sepharose beads, number of washes and washing conditions were among the parameters that were carefully optimized. Following the immunoprecipitation with Bcl-xL antibody, immune

complexes were resolved on SDS-polyacrylamide gel and immunoblotted with anti-Aven antibody. Immunoprecipitation was done with rabbit polyclonal antibody and immunoblotting was done with mouse monoclonal antibody. The Aven protein was 55KDa. In accordance with recent studies, coimmunoprecipitation assay revealed that Aven interaction with Bcl-xL did not change upon taxane treatment. In this study, the phosphorylation of Bcl-xL by taxane treatment in correlation with apoptosis type cell death were shown in both MCF-7 and MDA-MB-231 total cell extracts. The western blot analysis results that the band intensities of paclitaxel and docetaxel treated Bcl-xL immunoprecipitates immunoblotted with anti-Aven antibody were the same compared to control. We conclude that Aven also interacts with phosphorylated form of Bcl-xL. Basu and Haldar (2003) suggested that Bcl-xl phosphorylation may be a reason of taxol induced cell death in prostate cancer cell lines. In this study, although Aven levels were the same compared to control after 24 hours of drug treatment, induced Bcl-xl phosphorylation may be a result of apoptosis induction due to drug treatment.

Aven also binds to the CED-3 homology domain of Apaf-1, a 97 amino acid region that contains a single CARD. After the release of cytochrome c from the mitochondria, Apaf-1 is known to associate with itself to form oligomers and recruit procaspase-9 via CARD-domain interactions.[37,38] Chau et al. (2000) showed that Aven acts as a cell death regulator. In Bcl-xl knockout mutants they found that Aven interacts with Apaf-1 and inhibits the caspase activity. The inhibition of Apaf-1-mediated cell death suggests that Aven interferes with the interaction of procaspase-9 and Apaf-1 or at another step in apoptosome activation cascade.[21] Aven was also shown to impair the autoprocessing of caspase-9 after the addition of cytochrome c and dATP to cell extracts.[20] In addition, Aven inhibited the processing of caspase-3, which suggests that impaired activation of caspase-9 results in the failure of caspase-9 to activate caspase-3.[20] Therefore in a further study, to understand the mechanism of Aven as a cell death regulator, Apaf-1 and Aven interaction could be studied upon taxane treatment. Moreover, taxane-induced apoptosome complex formation and caspase-9 activation may be checked.

Overexpression of anti-apoptotic proteins such that Bcl-xL or Bcl-2 has been shown in a number of cell lines to be a potent protector of cellular apoptosis induced by antineoplastic agents [143-145]. Aven is also an antiapoptotic protein and overexpression of it could protect cells from apoptosis induced by chemotherapeutic

agents. To check this, cells were transfected by pSG-HA-Aven plasmid. Mock plasmid was generated from pSG-HA-Aven plasmid by cutting with XbaI and BamHI, and religation of the 4 Kb fragment. Mock transfection of the cells was also performed as a control. Total protein extraction was performed 24-48 hour posttransfection and it gave sufficient amount of protein. After careful optimization of transfection protocol, protein expression levels were checked by immunoblotting of total protein extracts with HA antibody. Expression levels were high and appropriate for immunoprecipitation. In the first place, immunoprecipitation with HA-antibody and immunoblotting with the same antibody was performed. Since heavy cahin of the primary antibody used during immunoblotting was 50 KDa, it obscured HA-Aven protein. Thus immunoprecipitation of HA-Aven could not be checked. Then immunoblotting was done with mouse monoclonal Aven antibody, since HA-antibody used for immunoprecipitation was rabbit polyclonal. However it was seen that endogenous Aven was also immunoprecipitaed with HA-antibody, because of the presence of Aven band in the mock-transfected cell extracts. This could be because of the lower stringency of the buffer used. Milder buffers may yield higher background, whereas high-stringent buffers can dissociate the interacting proteins from the immunoprecipitated complexes in Co-IP assays. For the future studies, high-stringent conditions during both cell lysis (increasing the CHAPS percentage in the buffer) and co-immunoprecipitation (eg. formation of immunocomplexes and subsequent washing steps in a high-stringent buffer) and addition of pre-clearing step with Protein G sepharose matrix are recommended as possible solutions.

After overexpression of Aven was performed, as a second strategy downregulation of Aven with anti-sense technology was tested. The use of siRNAs for downregulaion of genes is a very new technique. Fire and coworkers first reported it in *Caenorhabditis elegans* in 1998 [154]. They showed that double-stranded RNA (dsRNA) introduced into *Caenorhabditis elegans* blocked gene expression by a process of sequence-specific, post-transcriptional gene silencing (PTGS), which they termed RNA interference (RNAi) [154]. Since then, gene silencing by dsRNA has been established in plants, invertebrates, vertebrates and in mammals [155].

The molecular mechanism of downregulation of gene expression is such that siRNA incorporated into a multiprotein RNA-induced silencing complex (RISC), where the siRNA duplex is unwound, leaving the antisense strand to guide RISC to its

homologous mRNA targets for endonucleolytic cleavage [146, 156, 157, 158].

Inhibition of several targets using siRNA can suppress the growth of various cancer cells [147]. Despite these promising preclinical data, inhibiting a single target gene may be insufficient to optimally control tumour progression, because numerous genes are involved in tumour progression. In fact, the combined use of siRNAs with other methods, e.g. chemotherapy, is more active than siRNA monotherapy [148–151].

In this study, MCF-7 and MDA-MB-231 cells were transfected with 5 nmol of Hs_Aven_3_HP siRNA (Qiagen) with transfection reagent according to the manufacturer's instructions. The amount of transfection reagent was optimized for both cell lines. The gene silencing was checked on both RNA and protein level. The mRNA level of the Aven was determined first with one-step RT PCR, then as a quantitative determination real time RT PCR was used. Both techniques could be used, but quantitative RT PCR is the most sensitive technique for mRNA detection and qunatification. RT-PCR can be used to quantify mRNA levels from much smaller samples. In fact, this technique is sensitive enough to enable quantitation of RNA from a single cell.

Real-time PCR monitors the amount of amplicon as the reaction occurs. Usually, the amount of product is directly related to the fluorescence of a reporter dye. Because it detects the amount of product as the reaction progresses, real-time PCR provides a wide linear dynamic range, demonstrates high sensitivity, and is very quantitative. The initial amount of template DNA is inversely proportional to a parameter measured for each reaction, the threshold cycle (Ct). It does not require post-reaction processing (such as characterization by agarose gel electrophoresis).

SYBR Green-based detection is the least expensive and easiest method available for real-time PCR. Other methods (such as TaqMan) require an expensive third primer labeled with a dye and a quencher. SYBR Green specifically binds double-stranded DNA by intercalating between base pairs, and fluoresces only when bound to DNA. Detection of the fluorescent signal occurs during the PCR cycle at the end of either the annealing or the extension step when the greatest amount of double-stranded DNA product is present. However, SYBR Green detects any double-stranded DNA non-specifically. Therefore, the reaction must contain a combination of primers and master mix that only generates a single gene-specific amplicon without producing any non-specific secondary products.

For quantification of the mRNA, Ct values were interpolated from the standard curve to yield a copy number of each cDNA. The raw abundance of Aven was divided by β-actin values obtained from the same samples to derive a normalized value for each sample. Then fold change was calculated by dividing normalized value of the Aven to the normalized value of the control.

The inhibiton of Aven expression was 2.3 fold for MCF-7 cells and 1.7 fold for MDA-MB-231 cells. The amount of transfection reagent used for MCF-7 cells were higher than the MDA-MB-231 cells. Since MCF-7 cells were more resistant to transfection, the ratio of siRNA to transfection reagent was increased up to 1:10. This could be because of the transfection efficiency and/ or half life of the target protein. The half life of the protein may also affect gene silencing. The mRNA level of Aven in MCF-7 cells was lower compare to the MDA-MB-231 cells. This could be another reason for resistance to gene silencing. The presence of estrogen receptor could also affect the transfection efficiency.

After establishing the overexpression and downregulation of Aven protein, taxane induced apoptotic cell death was checked with M30 assay. M30-Apoptosense® is an ELISA based on the M30 monoclonal antibody [159] and therefore can be used for the quantitative detection of the M30 neo-epitope (CK18Asp396-NE) on CK18. As the M30 neo-epitope is only exposed after caspase-cleavage of CK18 [160], it represents a specific marker of apoptosis in epithelial cells. The M30-Apoptosense® ELISA measures the accumulation of a caspase cleavage product rather than proteolytic activity itself. The most frequent forms of cancer in humans arise from cells of simple epithelia and express cytokeratin 18 (CK18). The unique combination of high expression in most cancer cells, but not in non-epithelial (lymphoid) cells, and the apoptosis specific cleavage by caspases makes CK18 an ideal marker for monitoring apoptosis in human sera. Recent studies have indeed showed increased levels of caspase-cleaved CK18 (CK18Asp396-NE: M30 neo-epitope) in sera from cancer patients subjected to different treatment regimen [161-163].

Groos et al. (2003) showed that apoptosis determination via M-30 assay was more reliable than TUNEL assay, which is common apoptosis detection assay.[170] Therefore in present study, the apoptosis were determined with CK-18 levels using M30 assay. The increament in M30 levels after drug treatment compare to the control samples was calculated and tabulated as follows:

Table5.1 The increament of M30 antigen levels in MCF-7 cells.

MCF-7	Not- Transfected	Overexpression	Silencing
Cisplatin	2.2 ↑	1.5 ↑	2.5 ↑
Docetaxel	1.6 ↑	2.2 ↑	1.2 ↑
Paclitaxel	1.6 ↑	2.2 ↑	1

Table5.2 The increament of M30 antigen levels in MDA-MB-231 cells.

MDA-MB-231	Not-Transfected	Overexpression	Silencing
Cisplatin	3.3 ↑	3.9 ↑	1.4 ↑
Docetaxel	2.8 ↑	3.1 ↑	1.4 ↑
Paclitaxel	3.1 ↑	3.4 ↑	1.2 ↑

Aven overexpression has been shown to be protective against serum deprivation and spent medium exposure in CHO cells. However Aven expression was observed to be pro-apoptotic after Sindbis virus infection of CHO cell cultures [21]. In the present study, overexpression of Aven in MCF-7 cells seems to be sensitizing them against taxanes, whereas downregulation of Aven results in desensitization of cells. Because 1.6 fold increment was detected after taxane treatment of MCF-7 cells. The fold change in M30 levels increased to 2.2 when Aven was overexpressed and the fold change was decreased to 1.2 when Aven was downregulated. Cisplatin is a well-known DNA damaging agent and used as a positive control for apoptosis. It exerts its cytotoxicity via the formation of mono-, inter-, and intrastrand cisplatin-DNA adducts, which can ultimately result in cell cycle arrests at G_1, S, or G_2-M and the induction of apoptosis. [164-167] Cisplatin treatment of MCF-7 cells resulted in 2.2 fold change in M30 levels. The overexpression of Aven caused 1.5 fold increment in M30 levels after cisplatin treatment and downregulation resulted in 2.5 fold increment. All these results indicate that Aven acts as an anti-apoptotic protein against cisplatin induced apoptosis and it is pro-apoptotic in the case of taxanes induced apoptosis.

In MDA-MB-231 cells the apoptotic response to taxanes resulted in 3.1 and 2.8 fold increase in M30 antigen levels for paclitaxel and docetaxel respectively.

When Aven was overexpressed, this fold change was 3.1 and 3.4 for docetaxel and paclitaxel respectively.

Thus Aven overexpression could not induce more apoptotic cell death as in the case of MCF-7 cells. While downregulation of Aven results in less apoptotic cell death for taxanes since M30 levels increased by 1.4 and 1.2 fold for docetaxel and paclitaxel respecively. For cisplatin, the induction of apoptosis increased when cells overexpressed Aven. (by 3.9 fold in M30 levels) On the other hand, downregulation of Aven resulted in 1.4 fold increment in M30 levels. Hence less apoptotic cell death. The downregulation of Aven is protective against both taxanes and cisplatin induced apoptosis. Upregulation seemed to be protective but not as effective as in the case of MCF-7 cells.

Our data suggest that Aven is an extremely important protein in the set of pro- and antiapoptotic effector molecules that exist in breast cancer cells, and the relative sensitivity of these cells to cytotoxic chemotherapy seems to be a direct function of the level of its expression. In addition, experiments presented here further highlight the value of the antisense biotechnology, when used in what is hopefully an appropriate and rigorous manner, in the validation of gene function.

6. CONCLUSION

The study showed that taxane induced apoptosis does not affect endogeneous Aven expression in both MCF-7 and MDA-MB-231 cell lines. The interaction between Aven and Bcl-xL did not change upon taxanes treatment. Taxanes induced phosphorylation of Bcl-xL in both MCF-7 and MDA-MB-231 cell lines. Phosphorylation of Bcl-xL did not abolish Aven-Bcl-xL association. Overexpression of Aven in MCF-7 cells results in chemosensitization against taxanes, while downregulation causes desensitization of cells against taxanes. For cisplatin-induced apoptosis, Aven overexpression has a protective role, whereas downregulation makes cells more prone to apoptosis. In MDA-MB-231 cells, sensitivity against taxanes and cisplatin decrease when Aven is downregulated. Upregulation of Aven results in more apoptotic cell death upon taxane and cisplatin treatment, but not as effective as in the case of MCF-7 cells.

The possible mechanism for the regulation of apoptotic proteins after taxane treatment is shown in Figure 6.1. Taxanes induce phosphorylation of Bcl-xL, which inhibits its anti-apoptotic activity. On induction of apoptosis, mitochondrial permeability transition pores will be opened and cytochrome-c will be released which will trigger the apoptosome complex formation and cells will die. The role of Aven in this pathway is to bind both Bcl-xL and Apaf-1. The interaction of Aven with Apaf-1 inhibits caspase-9 activation, hence apoptosome complex formation is abrogated and cell survives.

Future studies aim to search for any possible involvement of Aven in taxane induced apoptosis. Understanding the role of Aven in breast cancer development by working on tissues coming from breast cancer patient's will help for interpreting *in vitro* data.

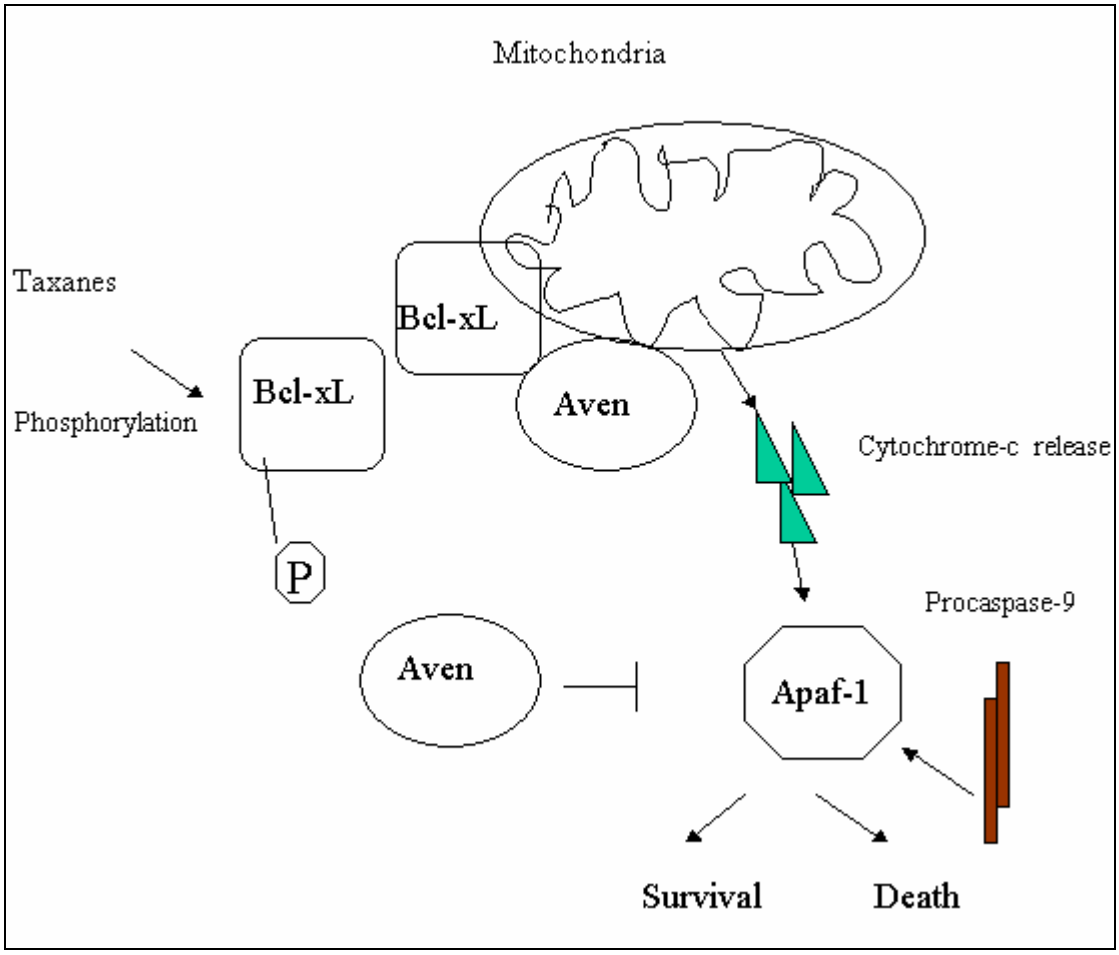

Figure 6. 1 Proposed mechanisms of Aven and interacting proteins.

7 REFERENCES

1. Tubiana-Hulin M. How to maximize the efficacy of taxanes in breast cancer. (2005) *Cancer Treat Rev.* **31:**3-9

2. Fitzpatrick FA, Wheeler R. The immunopharmacology of paclitaxel (TaxolR), docetaxel (TaxotereR), and related agents. (2003) *Int Immunopharmacol.* **3:**1699-171

3. Rowinsky EK. The development and clinical utility of the taxanes class of antimicrotubule chemotherapy agents. (1997) *Annu Rev Med.* **48:**353-374

4. Schiff PB, Fant J, Horwitz SB. Promotion of microtubule assembly in vitro by taxol. (1979) *Nature.* **277:**665-667.

5. Ringel I, Horwitz SB. Studies with RP 56976 (taxotere): a semisynthetic analogue of taxol. (1991) *J Natl. Cancer Inst.* **83:**288-291

6. Horwitz SB. Mechanism of action of taxol. (1992) *Trends Pharmacol Sci.* **13:**134-136.

7. Jordan MA,Wilson L. Microtubules and actin filaments: dynamic targets for cancer chemotherapy. (1998) *Curr Opin Cell Biol.* **10:**123-130.

8. Haldar S, Chintapalli J, Croce C.M. Taxol induces Bcl-2 phosphorylation and

death of prostate cancer cells. (1996) *Cancer Res.* **56:**1253-1255

9. Haldar S, Basu A, Croce C.M. Bcl2 is the guardian of microtubule integrity. (1997) *Cancer Res.* **57:**229-233

10. Haldar S, Jena N, Croce CM. Inactivation of Bcl-2 by phosphorylation. (1995) *Proc Natl Acad Sci USA.* **92:**4507-4511

11. Amato SF, Swart JM, Berg M, Wanebo HJ, Mehta SR, Chiles TC. Transient stimulation of the c-Jun-NH2-terminal kinase/activator protein 1 pathway and inhibition of extracellular signal-regulated kinase are early effects in paclitaxel-mediated apoptosis in human B lymphoblasts. (1998) *Cancer Res.* **58:**241-247.

12. Kim R, Ohi Y, Inoue H, Toge T. Taxotere activates transcription factor AP-1 in association with apoptotic cell death in gastric cancer cell lines. (1999) *Anticancer Res.* **19:**5399-5405.

13. Budman DR. Vinorelbine (Navelbine): a third-generation vinca alkaloid.(1997) *Cancer Invest*. **15:**475-490.

14. Green DR. Apoptotic pathways: paper wraps stone blunts scissors. (2000) *Cell.* **102:**1–4.

15. Wang X. The expanding role of mitochondria in apoptosis. (2001) *Genes Dev.* **15:**2922–2933.

16. Suzuki Y, Imai Y, Nakayama H, Takahashi K, Takio K, Takahashi R. A serine protease, Htra2, is released from the mitochondria and interacts with xiap, inducing cell death. (2001) *Mol Cell.* **8:**613–621.

17. Adams JM, Cory S. The Bcl-2 protein family: arbiters of cell survival. (1998) *Science.* **281:**1322–1326.

18. Huang DC, Strasser A. BH3-only proteins essential initiators of apoptotic cell death. (2000) *Cell.* **103:**839–842.

19. Martinou JC, Green DR. Breaking the mitochondrial barrier. (2001) *Nat Rev Mol Cell Biol.* **1:** 63–67.

20. Chau BN, Cheng EH, Kerr DA, Hardwick JM. Aven, a novel inhibitor of caspase activation, binds Bcl-xL and Apaf-1. (2000) *Mol Cell.* **6:**31-40

21. Figueroa BJr, Chen S, Oyler GA, Hardwick JM, Betenbaugh MJ. Aven and Bcl-xL enhance protection against apoptosis for mammalian cells exposed to various culture conditions. (2004) *Biotechnol Bioeng.* **85:**589-600

22. Gluecksmann A. Cell deaths in normal vertebrate ontogeny. (1951) *Biol. Rev.* **26**: 59-86.

23. Lockshin RA, Zakeri Z. Programmed cell death and apoptosis: origins of the theory. (2001) *Nat Rev Mol Cell Biol.* **2**: 545-550.

24. Lockshin RA, Williams CM. Programmed cell death.II Endocrine potentiation of the breakdown of the intersegmental muscles of silkmoths.(1964) *J Insect Physiol.* **10:**643-649

25. Kerr JF, Wyllie AH, Currie AR. Apoptosis: a basic biological phenomenon with wide-ranging implications in tissue kinetics.(1972) *Br J Cancer* **26:**239-57.

26. Fadeel B, Gleiss B, Hogstrand K, Chandra J, Wiedmer T, Sims PJ, Henter JI, Orrenius S and Samali A. Phosphatidylserine exposure during apoptosis is a cell-type-specific event and does not correlate with plasma membrane phospholipid scramblase expression.(1999) *Biochem Biophys Res Commun* **266:** 504-11.

27. Strasser A, O'Connor L, Dixit VM. Apoptosis signaling.(2000) *Annu Rev Biochem.* **69:**217-245

28. del Peso L, Gonzalez VM, Inohara N, Ellis RE, Nunez G.Disruption of the

CED-9 CED-4 complex by the EGL-1 is a critical step for programmed cell death in Caenorhabditis elegans.(2000) *J Biol Chem.* **275:**27205-27211.

29. Gewies A. Introduction to Apoptosis.(2003) *Aporeview*

30. Ashkenazi A, Dixit VM. Death receptors: signaling and modulation.(1998) *Science*. **281:** 1305-1308

31. Khosravi-Far R, Esposti MD. Death receptor signals to mitochondria.(2004) *Cancer Biol Ther*. **3:**1051-1057.

32. Ashkenazi A. Targeting death and decoy receptors of the tumour-necrosis factor superfamily.(2002) *Nat Rev Cancer* 2: 420-430.

33. Sun XM, MacFarlane M, Zhuang J, Wolf BB, Green DR, Cohen GM. Distinct caspase cascades are initiated in receptor-mediated and chemical-induced apoptosis.(1999) *J Biol Chem.* **274:**5053-5060.

34. Sprick MR, Weigand MA, Rieser E, Rauch CT, Juo P, Blenis J, Krammer PH, Walczak H. FADD/MORT1 and caspase-8 are recruited to TRAIL receptor 2.(2000) *Immunity* **12:**599-609

35. Bodmer JL, Holler N, Reynard S, Vinciguerra P, Schneider P, Juo P, Blenis J, Tschopp J. TRAIL receptor-2 signals apoptosis through FADD and caspase-8.(2000) *Nat Cell Biol.* **2:**241-243

36. Sartorius U, Schmitz I, Krammer PH. Molecular mechanisms of death-receptor-mediated apoptosis.(2001) *Chembiochem.* **2:**20-29.

37. Soderstrom TS, Poukkula M, Holmstrom TH, Heiskanen KM, Eriksson JE. Mitogen-activated protein kinase/extracellular signal-regulated kinase signaling in activated T cells abrogates TRAIL induced apoptosis upstream of the mitochondrial amplification loop and caspase-8.(2002) *J Immunol.* **169:** 2851-2860

38. Scaffidi C, Fulda S, Srinivasan A, Friesen C, Li F, Tomaselli KJ, Debatin KM, Krammer PH, Peter ME. Two CD95 (APO-1/Fas) signaling pathways. (1998) *EMBO J.* **17:**1675-1787

39. Ochs K, Kaina B. Apoptosis induced by DNA damage O6-methylguanine is Bcl-2 and caspase-9/3 regulated and Fas/caspase-8 independent. (2000) *Cancer Res*. **60:**5815-5824

40. Slee EA, Keogh SA, Martin SJ. Cleavage of BID during cytotoxic drug and UV radiation-induced apoptosis occurs downstream of the point of Bcl-2 action and is catalysed by caspase-3: a potential feedback loop for amplification of apoptosis-associated mitochondrial cytochrome c release. (2000) *Cell Death Differ.* **7:**556-565

41. de Moissac D, Gurevich RM, Zheng H, Singal PK, Kirshenbaum LA. Caspase activation and mitochondrial cytochrome c release during hypoxia-mediated apoptosis of adult ventricular myocytes. (2000) *J Mol Cell Cardiol.* **32:**53-63

42. van Grup M, Festjens N, van Loo G, Saelens X, Vandenabeele P. Mitochondrial intermembrane proteins in cell death. (2003) *Biochem Biophys Res Commun.* **304:** 487-497

43. Nguyen M, Millar DG, Yong VW, Korsmeyer SJ, Shore GC. Targeting of Bcl-2 to the mitochondrial outer membrane by a COOH-terminal signal anchor sequence.1993 *J Biol Chem.***268:**25265-25268

44. del Mar Martinez-Senac M, Corbalan-Garcia S, Gomez-Fernandez JC. Study of the secondary structure of the C-terminal domain of the antiapoptotic protein bcl-2 and its interaction with model membranes. (2000) *Biochemistry.* **39:**7744-7752

45. Sattler M, Liang H, Nettesheim D, Meadows RP, Harlan JE, Eberstadt M, Yoon HS, Shuker SB, Chang BS, Minn AJ, Thompson CB, Fesik SW. Structure of Bcl-xL-Bak peptide complex: recognition between regulators of apoptosis. (1997) *Science.* **275:**983-986

46. Hinds MG, Lackmann M, Skea GL, Harrison PJ, Huang DC,Day CL. The structure of Bcl-w reveals a role for the C-terminal residues in modulating biological activity.(2003) *EMBO J* **22:**1497-1507.

47. Wilson-Annan J, O'Reilly LA, Crawford SA, Hausmann G, Beaumont JG, Parma LP, Chen L, Lackmann M, Lithgow T, Hinds MG et al. Proapoptotic BH3-only proteins trigger membrane integration of prosurvival Bcl-w and neutralize its activity.(2003) *J Cell Biol*. **162:**877-887.

48. Jeong SY, Gaume B, Lee YJ, Hsu YT, Ryu SW, Yoon SH, Youle RJ: Bcl-xL sequesters its C-terminal membrane anchor in soluble, cytosolic homodimers. (2004) *EMBO J* **23:**2146-2155.

49. He H, Lam M, McCormick TS, Distelhorst CW. Maintenance of calcium homeostasis in the endoplasmic reticulum by Bcl-2. (1997) *J Cell Biol.* **138:** 1219-1228

50. Bogdanov MB, Ferrante RJ, Mueller G, Ramos LE, Martinou JC, Beal MF. Oxidative stress is attenuated in mice overexpressing BCL-2 (1999) *Neurosci Lett.* **262:**33-36

51. Mirkovic N, Voehringer DW, Story MD, McConkey DJ, McDonnell TJ, Meyn RE. Resistance to radiation-induced apoptosis in Bcl-2 expressing cells is reversed by depleting cellular thiols. (1997) *Oncogene* **15:**1461-1470

52. Decaudin D, Geley S, Hirsch T, Castedo M, Marchetti P, Macho A, Kofler R, Kroemer G. Bcl-2 and Bcl-xL antagonize the mitochondrial dysfunction preceding nuclear apoptosis induced by chemotherapeutic agents. (1997) *Cancer Res* **57:**62-67

53. Rokhlin OW, Guseva N, Tagiyev A, Knudson CM, Cohen MB. Bcl-2 oncoprotein protects the human prostatic carcinoma cell line PC3 from TRAIL-mediated apoptosis.(2001) *Oncogene.* **20:**2836-2843

54. Memon SA, Moreno MB, Petrak D, Zacharchuk CM.Bcl-2 blocks glucocorticoid- but not Fas- or activation-induced apoptosis in a T cell hybridoma. (1995) *J Immunol.***155:**4644-4652

55. Gazitt Y**,** Shaughnessy P, Montgomery W. Apoptosis-induced by TRAIL AND TNF-alpha in human multiple myeloma cells is not blocked by BCL-2. (1999) *Cytokine.* **11:**1010-1019

56. Veis DJ, Sorenson CM, Shutter JR, Korsmeyer SJ. Bcl-2-deficient mice demonstrate fulminant lymphoid apoptosis, polycystic kidneys, and hypopigmented hair. (1993) *Cell* **75:**229-240

57. Motoyama N, Wang F, Roth KA, Sawa H, Nakayama K, Nakayama K, Negishi I, Senju S, Zhang Q, Fujii S. Massive cell death of immature hematopoietic cells and neurons in Bcl-x-deficient mice. (1995) *Science.* **267:** 1506-1510

58. Ito T, Deng X, Carr B, May WS. Bcl-2 phosphorylation required for anti-apoptosis function. (1997) *J Biol Chem.* **272:**11671-11673

59 Yamamoto K, Ichijo H, Korsmeyer SJ. BCL-2 is phosphorylated and inactivated by an ASK1/Jun N-terminal protein kinase pathway normally activated at G(2)/M.(1999) *Mol Cell Biol.* **19:**8469-8478

60. Basu A, Haldar S. Identification of a novel Bcl-xL phosphorylation site regulating the sensitivity of taxol- or 2-methoxyestradiol-induced apoptosis. (2003) *FEBS Lett.* **538:**41-47.

61. Nechushtan A, Smith CL, Hsu YT, Youle RJ. Conformation of the Bax C-terminus regulates subcellular location and cell death.(1999) *EMBO J.* **18:**2330-2341.

62. Antonsson B, Montessuit S, Sanchez B, Martinou JC. Bax is present as a high molecular weight oligomer/complex in the mitochondrial membrane of apoptotic cells.(2001) *J Biol Chem.* **276:**11615-11623.

63. Griffiths GJ, Dubrez L, Morgan CP, Jones NA, Whitehouse J, Corfe BM, Dive C, Hickman JA. Cell damage-induced conformational changes of the pro-apoptotic protein Bak in vivo precede the onset of apoptosis. (1999) *J Cell Biol.* **144:**903-914.

64. Mandic A, Viktorsson K, Strandberg L, Heiden T, Hansson J, Linder S, Shoshan MC. Calpain-mediated Bid cleavage and calpain-independent Bak modulation: two separate pathways in cisplatin-induced apoptosis. (2002) *Mol Cell Biol.* **22:**3003-3013

65. Wei MC, Zong WX, Cheng EH, Lindsten T, Panoutsakopoulou V, Ross AJ, Roth KA, MacGregor GR, Thompson CB, Korsmeyer SJ. Proapoptotic BAX and BAK: a requisite gateway to mitochondrial dysfunction and death.(2001) *Science* **292:**727-730.

66. Deng Y, Lin Y, Wu X. TRAIL-induced apoptosis requires Bax-dependent mitochondrial release of Smac/DIABLO. (2002) *Genes Dev.* **16:**33-45.

67. Ruiz-Vela A, Opferman JT, Cheng EH, Korsmeyer SJ. Proapoptotic BAX and BAK control multiple initiator caspases. (2005) *EMBO Rep.* **6:**379-385.

68. Wood DE, Thomas A, Devi La, Berman Y, Beavis RC, Reed JC, Newcomb EW. Bax cleavage is mediated by calpain during drug-induced apoptosis.(1998) *Oncogene* **17:**1069-1078

69. Cao X, Deng X, May WS. Cleavage of Bax to p18 Bax accelerates stress-induced apoptosis, and a cathepsin-like protease may rapidly degrade p18 Bax.(2003) *Blood.* **102:**2605-2614.

70. Letai A. BH3 domains as BCL-2 inhibitors: prototype cancer therapeutics. (2003) *Expert Opin Biol Ther.* **3:**293-304.

71. Nakano K, Vousden KH. PUMA, a novel proapoptotic gene, is induced by p53.(2001) *Mol Cell.* **7:**683-694.

72. Oda E, Ohki R, Murasawa H, Nemoto J, Shibue T, Yamashita T, Tokino T, Taniguchi T, Tanaka N. Noxa, a BH3-only member of the Bcl-2 family and Candidate mediator of p53-induced apoptosis. (2000) *Science* **288:**1053-1058

73. Yu J, Zhang L, Hwang PM, Kinzler KW, Vogelstein B, Zhang L. PUMA induces the rapid apoptosis of colorectal cancer cells. (2001) *Mol Cell* **7:**673-682

74. Datta SR, Dudek H, Tao X, Masters S, Fu H, Gotoh Y, Greenberg ME. Akt phosphorylation of BAD couples survival signals to the cell-intrinsic death machinery.(1997) *Cell* **91:**231-241.

75. Datta SR, Katsov A, Hu L, Petros A, Fesik SW, Yaffe MB, Greenberg ME. 14-3-3 proteins and survival kinases cooperate to inactivate BAD by BH3 domain phosphorylation. (2000) *Mol Cell.* **6:**41-51.

76. Konishi Y, Lehtinen M, Donovan N, Bonni A. Cdc2 phosphorylation of BAD links the cell cycle to the cell death machinery. (2002) *Mol Cell.* **5:**1005-1016.

77. Donovan N, Becker EB, Konishi Y, Bonni A. JNK phosphorylation and activation of BAD couples the stress-activated signaling pathway to the cell death machinery.(2002) *J Biol Chem.* **277:**40944-40909.

78. Dramsi S, Scheid MP, Maiti A, Hojabrpour P, Chen X, Schubert K, Goodlett DR, Aebersold R, Duronio V. Identification of a novel phosphorylation site, Ser-170, as a regulator of bad pro-apoptotic activity. (2002) *J Biol Chem.* **277:**6399-6405

79. Verma S, Zhao LJ, Chinnadurai G. Phosphorylation of the pro-apoptotic protein BIK: mapping of phosphorylation sites and effect on apoptosis. (2001) *J Biol Chem*. **276:** 4671–4676.

80. Li H, Zhu H, Xu CJ, Yuan J.Cleavage of BID by caspase 8 mediates the mitochondrial damage in the Fas pathway of apoptosis. (1998) *Cell.* **94:** 491-501

81. Gross A, Yin XM, Wang K, Wei MC, Jockel J, Milliman C, Erdjument-Bromage H, Tempst P, Korsmeyer SJ. Caspase cleaved BID targets mitochondria and is required for cytochrome c release, while Bcl-xL prevents this release but not tumor necrosis factor-R1/Fas death.(1999) *J Biol Chem.* **274:** 1156-1163

82. Zha J, Weiler S, Oh KJ, Wei MC, Korsmeyer SJ. Posttranslational N-myristoylation of BID as a molecular switch for targeting mitochondria and apoptosis.(2000) *Science.* **290:**1761-1765

83. Alnemri ES, Livingston DJ, Nicholson DW, Salvesen G, Thornberry NA, Wong WW & Yuan J Human ICE／CED-3 protease nomenclature.(1996) *Cell* **87:**171.

84. Launay S, Hermine O, Fontenay M, Kroemer G, Solary E, Garrido C. Vital functions for lethal caspases.(2005) *Oncogene* **24:**5137−5148

85. Fan TJ, Han LH, Cong RS, Liang J. Caspase Family Proteases and Apoptosis. (2005) *Acta Biochim Biophys Sin*. **37:**719-727

86. Takahashi R, Deveraux Q, Tamm I, Welsh K, Assa-Munt N, Salvesen GS, Reed JC. A single BIR domain of XIAP sufficient for inhibiting caspases. (1998) *J Biol Chem* **273:**7787-7790.

87. Salvesen GS, Duckett CS. IAP proteins: blocking the road to death's door. (2002) *Nat Rev Mol Cell Biol* **3:** 401-410.

88. Huang Y, Park YC, Rich RL, Segal D, Myszka DG, Wu H. Structural basis of caspase inhibition by XIAP: differential roles of the linker versus the BIR domain. (2001) *Cell* **104:**781-90.

89. Srinivasula SM, Hegde R, Saleh A, Datta P, Shiozaki E, Chai J, Lee RA, Robbins PD, Fernandes-Alnemri T, Shi Y, Alnemri ES.A conserved XIAP-

interaction motif in caspase-9 and Smac/DIABLO regulates caspase activity and apoptosis.(2001) *Nature* **410:** 112-116.

90. Yang Y, Fang S, Jensen JP, Weissman AM, Ashwell JD. Ubiquitin protein ligase activity of IAPs and their degradation in proteasomes in response to apoptotic stimuli.(2000) *Science* **288:**874-877.

91. Huang H, Joazeiro CA, Bonfoco E, Kamada S, Leverson JD, Hunter T . The inhibitor of apoptosis, cIAP2, functions as a ubiquitin-protein ligase and promotes in vitro monoubiquitination of caspases 3 and 7.(2000) *J Biol Chem* **275:**26661-26664.

92. Suzuki Y, Nakabayashi Y, Nakata K, Reed JC, Takahashi R. X-linked inhibitor of apoptosis protein (XIAP) inhibits caspase-3 and -7 in distinct modes. (2001) *J Biol Chem* **276:** 27058-63.

93. Chai J, Du C, Wu JW, Kyin S, Wang X, Shi Y. Structural and biochemical basis of apoptotic activation by Smac/DIABLO. (2000) *Nature* **406:** 855–862.

94. Martins LM. The serine protease Omi/HtrA2: A second mammalian protein with a Reaper-like function. (2002) *Cell Death Differ.* **9:** 699–701.

95. Paydas S, Tanrıverdi K, Yavuz S, Disel U, Sahin B, Burgut R. Survivin and aven: two distinct antiapoptotic signals in acute leukemias. (2003) *Ann Oncol.* **14:**1045-1050

96. Pazdur R, Kudelka AP, Kavanagh JJ, Coh PR, Raber MN. The taxoids: paclitaxel (Taxol) and docetaxel (Taxotere). (1993) *Cancer Treat Rev*. **19:**351-386.

97. Jordan MA, Toso RJ, Thrower D, Wilson L. Mechanism of mitotic block and inhibition of cell proliferation by taxol at low concentrations. (1993) *Proc. Natl. Acad. Sci. USA*. **90:**9552-9556.

98. Schiff PB, Horowitz SB. Taxol stabilizes microtubules in mouse fibroblast cells. (1980) *Proc. Natl. Acad. Sci. USA*. **77:**1561-1565

99. Lavelle F, Bissery MC, Combeau C, Riou JF, Vrignaud P, Andre S. Preclinical evaluation of docetaxel (Taxotere). (1995) *Sem Oncol*. **22:**3-16

100. Von Hoff DD. The taxoids: same roots, different drugs. (1997) *Semin Oncol*. ***24*:**3-10

101. Ebneth A, Godemann R, Stamer K, Illenberger S, Trinczek B, Mandelkow EM, Mandelkow L. Overexpression of tau protein inhibits kinesin-dependent trafficking of vesicles, mitochondria, and endoplasmic reticulum: implications for Alzheimer's disease. (1998) *J Cell Biol*. **143:**777-794.

102. Wang LG, Liu XM, Kreis W, Budman DR. The effect of antimicrotubule agents on signal transduction pathways of apoptosis: a review.(1999) *Cancer Chemther Pharmacol*. **44:**355-361.

103. Scatena CD, Stewart ZA, Mays D, Tang LJ, Keefer CJ, Leach SD, Pietenpol JA. Mitotic phosphorylation of Bcl-2 during normal cell cycle progression and Taxol-induced growth arrest.(1998) *J Biol Chem*. **273:** 30777-30784

104. Stein CA. Mechanisms of action of taxanes in prostate cancer. (1999) *Semin. Oncol*. **26:** 3-7.

105. Blagosklonny MV, Fojo T. Molecular effects of paclitaxel: myths and reality (1999) *Int J Cancer.* **83:**151-156.

106. Reed JC. Double identity for proteins of the Bcl-2 family. (1997) *Nature* **387:**773-776.

107. Puthalakath H, Huang DC, O'Reilly LA, King SM, Strasser A. The proapoptotic activity of the Bcl-2 family member Bim is regulated by interaction with the dynein motor complex.(1999) *Mol Cell.* **3:**287-296

108. Srivastava RK, Mi QS, Hardwick JM, Longo DL. Deletion of the loop region of Bcl-2 completely blocks paclitaxel-induced apoptosis. (1999) *Proc. Natl. Acad. Sci. USA*. **96:** 3775-3780.

109. Evtodienko YV, Teplova VV, Sidashi SS, Ichas F, Mazat JP. Microtubule-active drugs suppress the closure of the permeability transition pore in tumour mitochondria. (1996) *FEBS Lett*. **393:** 86-88.

110. Rodi D, Janes R, Sangenee H, Holton RA, Wallace BA, Makowski L. Screening of a library of phage-displayed peptides identifies human bcl-2 as a taxol-binding protein. (1999) *J Mol Biol*. **285:**197-203.

111. Strobel T, Swanson L, Korsmeyer S, Cannistra SA. BAX enhances paclitaxel-induced apoptosis through a p53-independent pathway (1996) *Proc. Natl. Acad. Sci. USA*. **93:**14094-14099.

112. Kim R, Ohi Y, Inoue H, Toge T. Activation and the interaction of proapoptotic genes in modulating sensitivity to anticancer drugs in gastric cancer cells.(1999) *Int. J. Oncol*. **15:** 751-756.

113. Ling YH, Consoli U, Tornos C, Andreeff M, Perez-Soler R. Accumulation of cyclin B1, activation of cyclin B1-dependent kinase and induction of programmed cell death in human epidermoid carcinoma KB cells treated with taxol.(1998) *Int J Cancer.* **75:** 925-932.

114. Shimizu S, Eguchi Y, Kamiike W, Waguri S, Uchiyama Y, Matsuda H, Tsujimoto Y. Retardation of chemical hypoxia-induced necrotic cell death by Bcl-2 and ICE inhibitors: possible involvement of common mediators in apoptotic and necrotic signal transductions. (1996) *Oncogene* **12:** 2045-2050

115. Leist M, Nicotera P. Apoptosis, excitotoxicity, and neuropathology.(1998) *Exp. Cell Res*. **239:** 183-201

116. Heibein JA, Barry M, Motyka B, Bleackley C. Granzyme B-induced loss of mitochondrial inner membrane potential (Delta Psi m) and

cytochrome c release are caspase independent. (1999) *J. Immunol*. **163:** 4683-4693.

117. Eskes R, Antonsson B, Osen-Sand A, Montessuit S, Richter C, Sadoul R, Mazzei G, Nichols A, Martinou JC. Bax-induced cytochrome C release from mitochondria is independent of the permeability transition pore but highly dependent on Mg^{+2} ions.(1998) *J Cell Biol*. **143:** 217-224.

118. Yang XH, Sladek TL, Liu X, Butler BR, Froelich CJ, Thor AD. Reconstitution of caspase 3 sensitizes MCF-7 breast cancer cells to doxorubicin- and etoposide-induced apoptosis. (2001) *Cancer Res*. **61:** 348-354.

119. Ritter PM, Marti A, Blanc C, Baltzer A, Krajewski S, Reed JC, Jaggi R. Nuclear localization of procaspase-9 and processing by a caspase-3-like activity in mammary epithelial cells. (2000) *Eur J Cell Biol*. **79:**358-364.

120. Kottke TJ, Blajeski AL, Meng XW, Svingen PA, Ruchaud S, Mesner PW, Boerner SA, Samejima K, Henriquez NV, Chilcote TJ, Lord J, Salmon M, Earnshaw WC, Kaufmann SH. Lack of correlation between caspase activation and caspase activity assays in paclitaxel-treated MCF-7 breast cancer cells. (2002) *J Biol Chem*. **277:**804-815.

121. Ibrado AM, Kim CN, Bhalla K. Temporal relationship of CDK1 activation and mitotic arrest to cytosolic accumulation of cytochrome C and caspase-3 activity during Taxol-induced apoptosis of human AML HL-60 cells. (1998) *Leukemia*. **12:**1930-1936.

122. Panvichian R, Orth K, Day ML, Pienta KJ. Paclitaxel-associated multimininucleation is permitted by the inhibition of caspase activation: a potential early step in drug resistance. (1998) *Cancer Res* **58:** 4667-4672.

123. Gonçalves A, Braguer D, Carles G, André N, Prevôt C, Briand C. Caspase-8 activation independent of CD95/CD95-L interaction during paclitaxel-induced apoptosis in human colon cancer cells (HT29-D4). (2000) *Biochem Pharm*. **60**:1579-1584

124. Odoux C, Albers A, Amoscato AA, Lotze MT, Wong MK. TRAIL, FasL and a blocking anti-DR5 antibody augment paclitaxel-induced apoptosis in human non-small-cell lung cancer. (2002) *Int J Cancer*. **97:** 458-465

125. Fulda S, Susin SA, Kroemer G, Debatin KM. Molecular ordering of apoptosis induced by anticancer drugs in neuroblastoma cells. (1998) *Cancer Res*. **58:**4453-4460.

126. Ferrari D, Stepczynska A, Los M, Wesselborg S, Schulze-Osthoff K. Differential regulation and ATP requirement for caspase-8 and caspase-3 activation during CD95- and anticancer drug-induced apoptosis. (1998) *J Exp Med*. **188:** 979-984

127- Pucci B, Bellincampi L, Tafani M, Masciullo V, Melino G, Giordano A. Paclitaxel induces apoptosis in Saos-2 cells with CD95L upregulation and Bcl-2 phosphorylation. (1999) *Exp. Cell Res*. **252:**134-143

128- Wang S, Wang Z, Boise L, Dent P, Grant S. Loss of the bcl-2 phosphorylation loop domain increases resistance of human leukemia cells (U937) to paclitaxel-mediated mitochondrial dysfunction and apoptosis. (1999) *Biochem.Biophys*. **259:** 67-72.

129- Ibrado AM, Liu L, Bhalla K. Bcl-xL overexpression inhibits progression of molecular events leading to paclitaxel-induced apoptosis of human acute myeloid leukemia HL-60 cells. (1997) *Cancer Res*. **57:**1109-1115

130. Pastorino JG, Tafani M, Rothman RJ, Marcineviciute A, Hoek JB, Farber JL. Functional consequences of the sustained or transient activation by Bax of the mitochondrial permeability transition pore. (1999) *J Biol Chem*. **274:**31734-31739.

131. Rudner J, Lepple-Wienhues A, Budach W, Berschauer J, Friedrich B, Wesselborg S, Schulze-Osthoff K, Belka C. Wild-type, mitochondrial and ER-restricted Bcl-2 inhibit DNA damage-induced apoptosis but do not affect death receptor-induced apoptosis. (2001) *J Cell Sci*. **114:** 4161-4172

132. Minn AJ, Boise LH, Thompson CB. Expression of Bcl-xL and loss of p53 can cooperate to overcome a cell cycle checkpoint induced by mitotic spindle damage. (1996) *Genes Dev*. **10:** 2621-2631.

133. Ng FW, Shore GC. Bcl-XL cooperatively associates with the Bap31 complex in the endoplasmic reticulum, dependent on procaspase-8 and Ced-4 adaptor. (1998) *J. Biol. Chem*. **273:** 3140-3143.

134. Pienta KJ. Preclinical mechanisms of action of docetaxel and docetaxel combinations in prostate cancer. (2001) *Semin. Oncol*. ***28*:** 3-7

135. Muenchen HJ, Poncza PJ, Pienta KJ. Different docetaxel-induced apoptotic pathways are present in prostate cancer cell lines LNCaP and PC-3. (2001) *Urology*. **57:** 366-370

136. Escuin D, Rosell R. The anti-apoptosis survivin gene and its role in human cancer: an overview. (1999) *Clin Lung Cancer*. **1:**138-143

137. O'Connor DS, Grossman D, Plescia J, Li FZ, Zhang H, Villa A, Tognin S, Marchisio PC, Altieri DC. Regulation of apoptosis at cell division by p34cdc2 phosphorylation of survivin. (2000) *Proc. Natl. Acad. Sci. USA*. **97:** 13103-13107

138. Sintich S, Steinberg J, Kozlowski J, Lee C, Pruden S, Sayeed S, Sensibar JA. Cytotoxic sensitivity to tumor necrosis factor-alpha in PC3 and LNCaP prostatic cancer cells is regulated by extracellular levels of SGP-2 (clusterin). (1999) *Prostate*. ***39*:**87-93.

139. Li F, Ambrosini G, Chu E, Plescia J, Tognin S, Marchisio PC, Altieri DC. Control of apoptosis and mitotic spindle checkpoint by survivin. (1998) *Nature*. ***396*:** 580-584

140. Ding HF, Fisher DE. Induction of apoptosis in cancer: new therapeutic opportunities.(2002) *Ann Med.* **34:** 451–469

141. Hemann MT, Bric A, Teruya-Feldstein J, Herbst A, Nilsson JA, Cordon-Cardo

C, Cleveland JL, Tansey WP, Lowe SW.Evasion of the p53 tumor surveillance network by tumor-derived MYC mutants. (2005) *Nature.* **436:**807-811.

142. Zornig M, Hueber A, Baum W, Evan G. Apoptosis regulators and their role in tumorigenesis. (2001) *Biochim. Biophys. Acta.* **1551:** 1–37.

143. Minn AJ, Rudin C M, Boise LH, Thompson CB. Expression of bcl-xL can confer a multidrug resistance phenotype.(1995) *Blood*. **86:** 1903–1910.

144. Schmitt E, Steyaert A, Cimoli G, Bertrand R. Bax-a promotes apoptosisinduced by cancer chemotherapy and accelerates the activation of caspase 3-like cysteine proteases in p53 double mutant B lymphoma Namalwa cells. (1998) Cell Death Differ. 5: 506–516.

145. Wang S, Wang Z, Boise LH, Dent P, Grant S. Bryostatin 1 enhances paclitaxel-induced mitochondrial dysfunction and apoptosis in human leukemia cells (U937) ectopically expressing Bcl-xL. (1999) Leukemia. 13: 1564–1573.

146. Ji J, Wernli M, Klimkait T, Erb P. Enhanced gene silencing by the application of multiple specific small interfering RNAs. (2003) FEBS Lett. 552: 247–252.

147. Verma UN, Surabhi RM, Schmaltieg A,Becerra C, Gaynor RB. Small interfering RNAs directed against beta-catenin inhibit the in vitro and in vivo growth of colon cancer cells. (2003) Clin Cancer Res. 9: 1291–1300.

148. Zangemeister-Wittke U, Schenker T,Luedke GH, Stahel RA. Synergistic cytotoxicity of bcl-2 antisense oligodeoxynucleotides and etoposide, doxorubicin and cisplatin on small-cell lung cancer cell lines. (1998) Br J Cancer. 78: 1035–1042.

149. Miyake H, Nelson C, Rennie PS, Gleave ME. Acquisition of chemoresistant phenotype by overexpression of the antiapoptotic gene testosteronerepressed prostate message-2 in prostate cancer xenograft models.(2000) *Cancer Res.* **60:** 2547–2554.

150. Jansen B, Schlagbauer-Wadle H, Brown BD Bcl-2 antisense therapy chemosensitizes human melanoma in SCID mice. (1998) *Nat Med.* **4**: 232–234.

151. Miyake H, Tolcher A, Gleave ME. Chemosensitization and delayed androgen-independent recurrence of prostate cancer with the use of antisense Bcl-2 oligodeoxynucleotides. (2000) *J Natl Cancer Invest.* **92:** 34–41.

152. Soule HD, Vazquez J, Long A, Albert S, Brennan M. A human cell line from a pleural effusion derived from a breast carcinoma.(1973) *J Natl Cancer Inst.* **51:**1409–1416.

153. Cailleau R, Young R, Olive M, Reeves WJ Jr. Breast tumor cell lines from pleural effusions.(1974) *J Natl Cancer Inst.* **53:**661–674.

154. Fire A, Xu S, Montgomery MK, Kostas SA, Driver SE, Mello CC. Potent and specific genetic interference by double-stranded RNA in Caenorhabditis elegans. (1998) *Nature* **391:**806-811.

155. Sharp PA. RNA interference--2001. (2001) *Genes Dev.* **15:** 485-490.

156. Zamore PD. Ancient pathways programmed by small RNAs. (2002) *Science* **296:** 1265-1269.

157. Plasterk RH. RNA silencing: the genome's immune system. (2002) *Science* **296:** 1263-1265.

158. Dykxhoorn DM, Novina CD, Sharp PA. Killing the messenger: short RNAs that silence gene expression. (2003) *Nat.Rev. Mol. Cell Biol.* **4:**457-467.

159. Leers MP, Kolgen W, Bjorklund V, Bergman T, Tribbick G, Persson B, Bjorklund P, Ramaekers FC, Bjorklund B, Nap M, Jornvall H, Schutte B. Imunocytochemical detection and mapping of a cytokeratin 18 neo-epitope exposed during early apoptosis.(1999) *J Pathol.* **187:**567-572.

160. Hagg M, Biven K, Ueno T, Rydlander L, Bjorklund P, Wiman KG, Shoshan M, Linder S. A novel high-through-put assay for screening of pro-apoptotic drugs. (2002) *Invest New Drugs.* **20:**253-259.

161. Ueno T, Toi M, Bivén K, Bando H, Ogawa T, Linder S. Measurement of an apoptosis product in the sera of breast cancer patients. (2003) *Eu. J Cancer.* **39:** 769-774.

162. Bivén K, Erdal H, Hägg M, Ueno T, Zhou R, Lynch M, Rowley B, Wood J, Zhang C, Toi M, Shoshan MC, Linder S. A novel assay for discovery and characterization of pro-apoptotic drugs and for monitoring apoptosis in patient sera. (2003) *Apoptosis* **8:** 263-268.

163. Kramer G, Erdal H, Mertens H, Nap M, Mauermann J, Steiner G, Marberger M, Biven K, Shoshan MC, Linder S. erentiation between Cell Death Modes using Measurements of Different Soluble Forms of Extracellular Cytokeratin 18. (2004) *Cancer Res.* **64:** 1751-1756.

164. Fichtinger-Schepman AM, van der Veer JL, den Hartog JH, Lohman PH, and Reedijk J. Adducts of the antitumor drug *cis*-diamminedichloroplatinum(II) with DNA: formation, identification, and quantitation. (1985) *Biochemistry.* **24:** 707–713.

165. Sorenson CM, Eastman A. Influence of *cis*-diamminedichloroplatinum(II) on DNA synthesis and cell cycle progression in excision repair proficient and deficient Chinese hamster ovary cells. (1998) *Cancer Res.* **48:** 6703–6707.

166. Wyllie AH, Kerr JF, Currie AR. Cell death: the significance of apoptosis. (1980) Int Rev Cytol. **68:** 251–306.

167. Vaisman A, Varchenko M, Said I, Chaney SG. Cell cycle changes associated with formation of Pt-DNA adducts in human ovarian carcinoma cells with different cisplatin sensitivity. (1997) Cytometry. **27:** 54–64.

168. Schutte B, Henfling M, Kolgen W, Bouman M, Meex S, Leers MP, Nap M, Bjorklund V, Bjorklund P, Bjorklund B, Lane EB, Omary MB, Jornvall H, Ramaekers FC. Keratin 8/18 breakdown and reorganization during apoptosis.(2004) *Exp Cell Res*. **297:** 11-26.

169. Ganansia-Leymarie V, Bischoff P, Bergerat JP, Holl V. Signal Transduction Pathways of Taxanes-Induced Apoptosis. (2003) *Curr. Med. Chem.* **3:**291-306

170. Groos S, Reale E, Luciano L.General suitability of techniques for in situ detection of apoptosis in small intestinal epithelium.(2003) *Ant. Rec.A Discov Mol Cell Evol Biol.* **272:**503-513

APPENDIX A

CHEMICALS

(in alphabetical order)

Name of Chemical	Supplier Company	Catalog Number
Acrylamide/Bisacrylamide(30%)	Sigma, Germany	A3699
Agarose low EEO	AppliChem, Germany	A2114
Ammonium persulfate	Sigma, Germany	A3678
Ampicillin	Sigma, Germany	A9518
Anti-Aven Ab	BD, USA	A21820
Anti-β-actin Ab	Abcam, UK	6276
Anti-BcL-XL Ab	Cell Signal Tech., USA	2762
Anti-HA Ab	Abcam, UK	9110
Bradford Solution	Biorad Inc., USA	500-0001
BSA(blot-qualified)	Promega, USA	W384A
CHAPS	Amresco, USA	75621
Coomassie Brilliant Blue	Merck, Germany	115444
Developer solution	Agfa, USA	G150
DMSO (tissue-culture grade)	Sigma, Germany	D2650
EDTA	Sigma, Germany	E5134
EGTA	Fluka, Germany	O3780
Ethanol	Merck, Germany	100986
Ethidium Bromide	Merck, Germany	OCO28942
FCS/FBS	Biological Industries, Israel	04-121-1A
Fixer solution	Agfa, USA	601084
Glycine	Amresco, USA	0167
HCl	Merck, Germany	100314

Hyperfilm ECL	Amersham Bio., UK	RPN2114K
Isopropanol(2-propanol)	Riedel-de Haen, Germany	24137
Liquid Nitrogen	Karbogaz, Turkey	
LB Agar	Sigma, Germany	L-3147
LB Broth	Sigma, Germany	L-3022
L-glutamine	Merck, Germany	100289
2-Mercaptoethanol	Sigma, Germany	M370-1
Methanol	Riedel-de Haen, Germany	24229
$MgCl_2.6H_2O$	Sigma, Germany	M9272
Milk Diluent concentrate	KPL, USA	50-82-00
NaCl	Riedel-de Haen, Germany	13423
NaF	Sigma, Germany	S1504
Na_3VO_4	Sigma, Germany	S6508
$C_{24}H_{39}NaO_4.H_2O$	Sigma, Germany	D6740
NaOH	Merck, Germany	106462
Non-fat dry milk	Pinar, Turkey	
NP-40 (IGEPAL CA-630)	Calbiochem, Germany	492015
PBS (10X)	Biological Industries, Israel	02-023-5A
PBS (1X)	Biological Industries, Israel	02-023 -1A
Phenol	Applichem, Germany	A1153
Penicillin/Streptomycin	Biological Industries, Israel	03-031-1B
PMSF	Sigma, Germany	P7626
RPMI-1640	Biological Industries, Israel	01-106-1A
SDS	Sigma, USA	L4390
TEMED	Sigma, Germany	T7029
Tris base	Amresco, USA	0826500G
Trypsin/EDTA(1X)	Biological Industries, Israel	03-053-1A
Tween-20™	Merck, Germany	822184

APPENDIX B

MOLECULAR BIOLOGY KITS

(in alphabetical order)

Name of Kit	Supplier Company	Catalog Number
ECL Advance Chemiluminescence Detection Kit	Amersham Biosci., UK	RPN2135
Cell Proliferation Kit I (MTT)	Roche, Germany	1465007-001
Hiperfect Transfection Reagent	Qiagen, Germany	301704
M30-Apoptosense® ELISA	Peviva, Sweden	PE0024
QIAGEN® Plasmid Midi Kit (100)	Qiagen, Germany	12145
One-step RT PCR Kit	Qiagen, Germany	210210
Quantitec SYBR green PCR Kit	Qiagen, Germany	204143

APPENDIX C

OTHER MATERIALS

(in alphabetical order)

Name of Material	**Supplier Company**	**Catalog Number**
Biomax 18X24, Int. Scr. Cassettes	Kodak, USA	
Complete™ protease inh. coc. tab.	Roche, Germany	11697498001
DNA Loading Dye(6X)	Fermentas, Germany	R0621
Electroporation cuvettes, 4 mm	BTX, USA	640
Flat gel-loading tips	Rainin, USA	GT-250-4
Fugene 6™ transfection reagent	Roche , Germany	11814443001
Protein G Sepharose™ 4 Fast Flow	Amersham Biosciences, UK	17-0618-01
GeneRuler™ 1 kb DNA Ladder	Fermentas,Germany	SM0311
Hybond-P membrane (PVDF)	Amersham Biosciences, UK	RPN2020F
Hyperfilm ECL	Amersham Biosciences, UK	RPN2103K
Full Range Rainbow™ Molecular Weight Marker	Amersham Biosciences, UK	RPN800
RNAse A	Roche, Germany	1119915
Restriction Endonucleases	Fermentas, GERMANY	ER0501
(BamH I, Hind III,		
T4 DNA Ligase	Promega,GERMANY	M180B
Klenow Fragment	Fermentas, GERMANY	

APPENDIX D

Autoclave:	Hirayama, Hiclave HV-110, JAPAN
	Certoclav, CV-EL-12L, AUSTRIA
Balance:	Sartorius;BP211D,BP221S,BP610, GERMANY
	Shimadzu, EB-3200, JAPAN
Blot Module:	Novex, X-Cell II^{TM} Blot, Invitrogen, USA
Centrifuge:	Kendro Lab. Prod., Heraeus 3L, GERMANY
	Hitachi, Sorvall RC5C Plus, USA
	Eppendorf; 5415D, 5415R, GERMANY
Deepfreezer:	-80^{o}C, Kendro Lab. Prod., Heraeus, GERMANY
	-20^{o}C, Bosch, TURKEY
Distilled Water:	Millipore, Elix-S, FRANCE
	Millipore, MilliQ Academic, FRANCE
Electroporator:	BTX, ECM 630, USA
Electrophoresis:	Bio-Rad Inc., Mini-Protean, USA
	Biogen Inc., DNA electrophoresis, USA
Gel Documentation:	Uvitec, UVIdoc, Biolab, UK
	Bio-Rad Inc., UV-Transilluminator, USA
Hematocytometer:	
Ice Machine:	Scotsman Inc., AF20, USA
Incubator:	Binder, CO_2 Incubator, GERMANY
Laminar Flow:	Kendro Lab. Prod., Heraeus, HeraSafe HS12, GERMANY
Magnetic Stirrer/Heater:	VELP Scientifica, ITALY
Microscope:	Olympus, CK40-F200, JAPAN
	Olympus, IX70, Phase-Contrast Fluorescence,JAPAN

Microwave Oven:	Bosch, TURKEY
pH-Meter:	Fisherbrand, Hydrus 300, UK
Pipette:	Ependorf, Research, GERMANY
	Mettler Toledo, Volumate, USA
	Gilson, Pipetman, FRANCE
	Pipetus-Akku, Hirschmann Laborgerate, GERMANY
Power Supply:	Wealtec, Elite 300, USA
	Biorad Inc., PowerPac 300, GERMANY
Refrigerator:	+4^{o}C, Bosch, TURKEY
Rotator:	Lab-Line Multitube Rotator, USA
	Labquake, Barnstead Thermolyne Corp.,
USA Shaker:	IKA, Orbital Shaker KS 260 basic, USA
	New Brunswick Sci., Innova^{TM} 4330, USA
Spectrophotometer:	Bio-Rad Inc., Microplate reader Model 680,USA
	Shimadzu,UV-3150, JAPAN
Tissue-Cell Culture Products:	TPP, SWITZERLAND
Thermocycler:	Eppendorf Master Cycler Gradient
	Biorad Icycler IQ
Vortex Mixer:	Velp Scientifica, 2x^{3}, ITALY
Water-bath:	Eppendorf, Thermomixer Comfort, GERMANY
	Huber, Polystat cc1, GERMANY